

# Changepoint Detection on a Graph of Time Series

Karl L. Hallgren<sup>1\*</sup>, Nicholas A. Heard<sup>1</sup> and Melissa J. Turcotte<sup>2</sup>

<sup>1</sup>Department of Mathematics, Imperial College London

<sup>2</sup>Microsoft Corporation

## Abstract

When analysing multiple time series that may be subject to changepoints, it is sometimes possible to specify *a priori*, by means of a graph, which pairs of time series are likely to be impacted by simultaneous changepoints. This article proposes an informative prior for changepoints which encodes the information contained in the graph, inducing a changepoint model for multiple time series that borrows strength across clusters of connected time series to detect weak signals for synchronous changepoints. The graphical model for changepoints is further extended to allow dependence between nearby but not necessarily synchronous changepoints across neighbouring time series in the graph. A novel reversible jump Markov chain Monte Carlo (MCMC) algorithm making use of auxiliary variables is proposed to sample from the graphical changepoint model. The merit of the proposed approach is demonstrated through a changepoint analysis of computer network authentication logs from Los Alamos National Laboratory (LANL), demonstrating an improvement at detecting weak signals for network intrusions across users linked by network connectivity, whilst limiting the number of false alerts.

*Keywords:* changepoint detection; graphical model; informative prior; auxiliary variable MCMC; cyber-security.

## 1. Introduction

Consider  $N > 1$  time series of random observations

$$\{x_{i,t} \mid 1 \leq i \leq N, t \geq 0\} \quad (1)$$

which are subject to changepoints. This article will suppose the existence of an underlying graph  $G$  on  $N$  nodes corresponding to each of the time series, such that changepoints are believed to occur simultaneously or closely together in time for time series connected by edges in  $G$ .

A motivating application for considering such dependencies is the task of changepoint detection in cyber-security. To identify the presence of a network intrusion, it is informative to monitor for changes in the authentication activity of each user in the network. However, cyber data often exhibit much variability and apparent changes are not guaranteed to correspond to an attack. As a result, to limit the number of false alerts and yet not overlook weak signals from genuine, small attack footprints, it is key to incorporate expert knowledge in the change detection procedure. A commonly held belief of security experts is that attacks are *a priori* likely to be identified through quasi-simultaneous changes in the behaviour of users that are linked by network connectivity (Sexton et al., 2015). Hence, it is of interest to encode a changepoint prior by means of a graph  $G$  representing the network of users, such that pairs of connected users in  $G$  are *a priori* more likely to be affected by quasi-simultaneous behavioural changes.

---

\*Email: karl.hallgren17@imperial.ac.uk

Limited attention has previously been given to encoding prior beliefs on graph-based dependence structure of discrete-time changepoints across multiple time series. Existing changepoint model for multiple time series, which admit changepoints may simultaneously affect a subset of the time series, typically assume *a priori* changepoint locations are exchangeable across time series (Jeng et al., 2012; Bardwell and Fearnhead, 2017; Bolton and Heard, 2018; Wang and Samworth, 2018; Bardwell et al., 2019; Grundy et al., 2020). Moreover, with the exception of Fisch et al. (2022), dependent changepoints across time series are often assumed to perfectly align, which is a limiting assumption in cyber-security monitoring where attacks may span a substantial period of time.

More generally, graphical models provide a useful framework for characterising joint distributions for random variables: the nodes of the graph identify the random variables and the edges characterise dependencies among these variables (Lauritzen, 1996). In particular, graphical models have been employed to encode prior beliefs, for example, in the context of Bayesian variable selection for regression models. Li and Zhang (2010) assumes that covariates lie on an undirected graph and formulates an Ising model prior on the covariate space to incorporate structural information.

This article proposes an informative, graphical model-based prior for changepoints that encodes beliefs on the dependence structure of changepoints across time series (1). For practical purposes, changepoints are represented in discrete time by a binary matrix  $S = (S_{i,t})$ , such that  $S_{i,t}$  indicates whether the time point  $t$  is a changepoint for the time series with index  $i$ . Then, extending the standard memoryless prior for changepoints (Fearnhead, 2006), independent and identical Markov random fields (Lauritzen, 1996) with respect to  $G$  are assumed *a priori* for the columns of  $S$ . As a result, the model assumes that clusters of time series (according to  $G$ ) are likely to be simultaneously affected by changepoints. Conditional on changepoints, the time series data are assumed to be independent of  $G$  and to follow a standard parameteric changepoint model (Fearnhead, 2006). A key consequence of the graphical model is that stronger evidence from data is required to infer scattered synchronous changepoints than synchronous changepoints clustered according to  $G$ . Furthermore, a more general model is proposed that admits related changepoints not occurring at exactly the same time; the extended model supposes that changepoints may cluster according to  $G$  within some finite time windows of possibly unknown lengths, which are specific to each series.

A common approach to sampling changepoints for a single time series is that of Green (1995), using a reversible jump MCMC algorithm to explore the state space of changepoints: at each iteration of the algorithm, a new changepoint is proposed, or else an existing changepoint is either deleted or shifted to a new position. Specifying a joint model for dependent changepoints across multiple time series introduces additional computational challenges that are not present when changepoints are inferred for each time series independently. A simulation study will demonstrate that it can be impractical to simply propose updates to the changepoints of a randomly chosen time series via one of the moves of Green (1995). To efficiently explore the state space of dependent changepoints, it is necessary to consider joint proposals for changepoints across multiple time series.

We propose an MCMC algorithm making use of auxiliary variables (Besag and Green, 1993) to sample from the posterior distribution. Swendsen and Wang (1987) and Higdon (1998) provide notable examples of use of auxiliary variables in MCMC schemes that improve mixing and convergence for undirected graphical models. In brief, our sampling strategy is the following. The changepoint parameter space is augmented with auxiliary variables that induce clusters of time series according to the dependence graph  $G$ . Then, the MCMC algorithm of Green (1995) is extended to sample from the augmented parameter space, such that, at each iteration of the algorithm, a new cluster of changepoints may be proposed or an existing cluster of changepoints may be deleted or shifted.

Bayesian inference for changepoints quantifies uncertainty about the number and the positions of changepoints. However, in some applications such as cyber-security, it will also be necessary to report a point estimate for changepoint parameters. Yet no existing loss function in the literature seems suitable for taking into account both the number and the positions of changepoints. To address this gap, we propose using matchings in graphs (Bondy and Murty, 1976) to define a novel loss function for changepoints, which can be used to obtain a point estimate from a posterior sample of candidate changepoints.

The practical benefits of the proposed graphical model are demonstrated via a changepoint analysis of real computer network authentication data from Los Alamos National Laboratory (LANL), where a subset of the data relating to a ‘red team’ exercise provide a proxy for intruder behaviour (Kent, 2015). The challenge consists of monitoring for temporal changes in the authentication activity of network users to detect the presence of red team actors. The proposed changepoint prior is used to encode beliefs that signals for network intrusions are *a priori* likely to occur at nearby times for users historically linked by previous network connectivity. We show that, as a consequence, the proposed model can detect weak signals for red team activity in the network, whilst limiting the number of false alerts, in contrast with a standard model assuming independence of behavioural changes across users.

Finally, it should be noted that, in contrast with recent changepoint detection methods (Chen and Zhang, 2015; Chen, 2019a,b; Chu and Chen, 2019), the focus of this article is not the temporal evolution of a graph subject to changepoints. The graph  $G$  represents prior information that can be exploited to detect changepoints in time series.

The remainder of the article is organised as follows. Section 2 motivates our work with a cyber-security application. Section 3 presents Bayesian changepoint modelling for multiple time series. Section 4 introduces a novel, graph-based informative prior for changepoints. Section 5 proposes an auxiliary variable MCMC sampling strategy. Section 6 proposes a novel loss function for assessing changepoints. Section 7 presents results of a changepoint analysis of network authentication data, illustrating the practical benefits of the proposed model. Appendices A, B and C present some technical material, and a simulation study in Appendix D demonstrates the model introduced in Section 4.

## 2. Motivational application: changepoint detection in cyber-security

To motivate an informative graph-based prior for changepoints, we consider an application of changepoint detection in cyber-security. A cyber-attack typically changes the behaviour of connected endpoints on the target computer network (Sexton et al., 2015). Therefore, to detect the presence of a network intrusion, it is informative to monitor for synchronous, or quasi-synchronous, changes in the behaviour of entities that are *a priori* known to be linked by network connectivity.

### 2.1. Change detection in the authentication activity of users

Kent (2015) presents a comprehensive data set summarising 58 days of traffic on the enterprise computer network of Los Alamos National Laboratory (LANL), which is available online at <https://lanl.ma.ic.ac.uk/data/cyber1>. The network authentication data consist of records describing authentication activity of users connecting from one computer to another. The occurrence of a ‘red team’ penetration testing operation during the data collection period makes these data suitable for testing network intrusion detection methods. Further details on the data are given in Appendix A.1.

Let  $V$  denote the set of users in the enterprise. To detect occurrences of malicious activity in the network, the authentication activity of each user  $i \in V$  is monitored via hourly counts of network logons per source computer. Let  $M$  denote the number of distinct source computers in

the network. For each user  $i \in V$ , let

$$x_{i,t} = (x_{i,t,1}, \dots, x_{i,t,M}), \quad (2)$$

where  $x_{i,t,\ell}$  denotes the number of network logons initiated by user  $i$  from source computer  $\ell$  during the  $t$ -th hour of the 58 day data collection period. For each user, it is of interest to detect temporal changes in the distribution of network logons across source computers as possible evidence for malicious activity. Figure 6 in Appendix A displays the authentication data for two users.

## 2.2. Motivation for an informative graph-based changepoint prior

The authentication data (2) exhibit much variability, and some observed changes can correspond to legitimate activity. Therefore, to limit the number of false alerts and yet not overlook weak signals from genuine attack footprints, it is key to incorporate prior knowledge in the change detection procedure.

When attackers penetrate a network, they rarely gain access to the target users directly; instead, they typically take control of a vulnerable user, for example via email phishing, and then they move laterally through the network, gaining access and compromising additional users, to achieve their objectives (Sexton et al., 2015). Attackers are typically constrained in the way they can navigate the network, and it will often be possible for cyber-security experts to specify a graph  $G = (V, E)$ , where an edge  $(i, i') \in E \subseteq V \times V$  indicates it is believed *a priori* that attackers may switch credentials between user  $i$  and user  $i'$  at any time during the data collection period. Therefore, it is of interest to encode in the changepoint prior that cyber-attacks are *a priori* likely to result in quasi-synchronous changes in the authentication activity of multiple users that are connected in  $G$ . In this article, we consider the following specification of  $G$  for demonstration purposes:  $(i, i') \in E$  if and only if both user  $i$  and user  $i'$  successfully initiated a network logon from the same source computer on the same day. This choice follows from the following considerations. In Windows operating systems, when a user logs on with their credentials (username and password hash) to a device on the domain, these credentials are cached locally on the device. Credential caching prevents users from continuously having to re-authenticate (single sign-on), and enables them to log on to the device even if the device is disconnected from the network. Attackers will exploit credentials which are cached on devices to upgrade their privileges and move laterally through the network. How long credentials may be cached on devices depends on the enterprise’s network settings. In the absence of precise knowledge about the enterprise’s network settings, it is reasonable to assume that if both user  $i$  and user  $i'$  have logged into a device on the same day then both those credentials may be cached on that device during the data collection period. As a result, if attackers had access to that device then they would have the ability to exploit cached credentials to switch credentials between user  $i$  and user  $i'$ .

In Figure 1, for the application of interest, each arrow corresponds to the authentication activity of a user on the network, and shaded rectangles indicate which pairs of users are connected in  $G$  and therefore likely to be impacted by simultaneous changes during an attack. It is of interest to encode in the changepoint prior, by means of the graph  $G$ , that pairs of users  $(i, i') \in E$  are likely to be simultaneously affected by malicious behavioural changes, thereby inducing a changepoint model for the authentication data that borrows strength across connected users in  $G$  to detect signals for clusters of synchronous changes, as sketched in Figure 1.

In contrast with recent intrusion detection methods (Chen and Zhang, 2015; Chen, 2019a; Metelli and Heard, 2019; Passino et al., 2021), the focus of this article is not the temporal evolution of a graph representing a network, and both  $V$  and  $E$  are constant in time. The graph  $G$  represents the best available static characterisation of the network that can be used to guide change detection in the authentication activity of users (2), and it is assumed to be readily

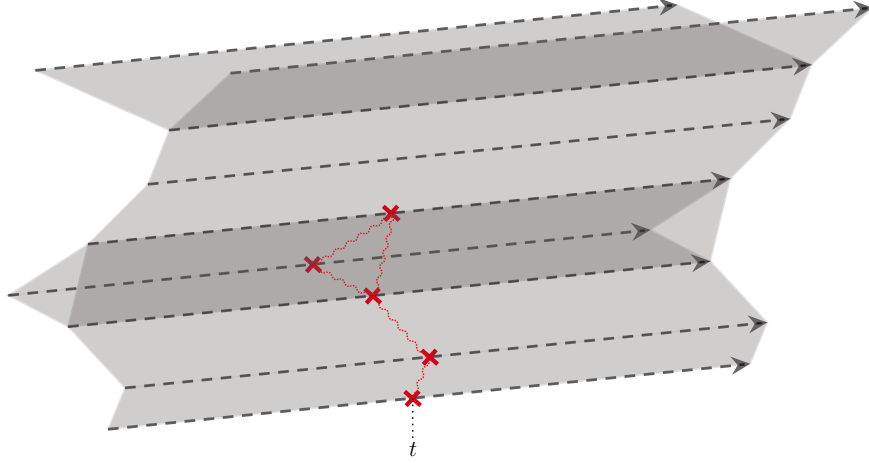


Figure 1: Cartoon representation of a cluster of synchronous changepoints (red crosses) on a graph of time series. Arrows represent time series, and shaded rectangles indicate which pairs of time series are likely to be impacted by simultaneous changepoints.

available prior to running network intrusion detection methods; note that, in practice, the edge set could be derived from historic data. Section 8 discusses possible model extensions for settings where prior beliefs on which time series are likely to be impacted by simultaneous changepoints may be time-dependent.

### 3. Changepoint analysis for multiple time series

Let  $G = (V, E)$  be a graph with node set  $V = \{1, \dots, N\}$  and edge set  $E \subseteq V \times V$ . For each node  $i \in V$  we observe a time series  $\mathbf{x}_i = (x_{i,0}, \dots, x_{i,T})$  which may be subject to changepoints, and the edge set  $E \subseteq V \times V$  indicates which pairs of time series are *a priori* likely to be impacted by quasi-simultaneous changepoints. Conditionally on changepoints, the data are assumed to be independent of  $G$  and follow a standard parametric changepoint model, presented in this section. Some limitations of the usual prior for independent changepoints are discussed, paving the way for the proposed informative prior for graph-dependent changepoints.

#### 3.1. Model and notation

For each node  $i \in V$ , suppose there are  $k_i \geq 0$  changepoints that partition the time series of observations for that node into  $k_i + 1$  segments. The ordered locations of the changepoints, denoted by  $\boldsymbol{\tau}_i = (\tau_{i,1}, \dots, \tau_{i,k_i})$ , belong to the set  $\mathcal{T}_{k_i}$ , where

$$\mathcal{T}_k = \left\{ (\tau_1, \dots, \tau_k) \in \mathbb{N}^k; 0 \equiv \tau_0 < \tau_1 < \dots < \tau_k < \tau_{k+1} \equiv T + 1 \right\}. \quad (3)$$

For each node  $i$ , the data  $x_{\tau_{i,j-1}}, \dots, x_{\tau_{i,j}-1}$  in each segment  $j$  are assumed to be drawn from a distribution from the same parametric family  $L_i(\cdot | \theta_{i,j})$ , with a segment specific parameter  $\theta_{i,j}$  drawn independently from a prior density  $\pi_i(\cdot)$ .

The parameters of interest are the changepoint parameters  $(\mathbf{k}, \boldsymbol{\tau})$ , where  $\mathbf{k} = (k_i)_{i \in V}$  and  $\boldsymbol{\tau} = (\boldsymbol{\tau}_i)_{i \in V}$ . Motivated by computational considerations, as in Fearnhead (2006) it is assumed in this article that segment parameters may be marginalised so that the likelihood of the data  $\mathbf{x}$  conditional on changepoints,

$$\mathcal{L}(\mathbf{x} | \mathbf{k}, \boldsymbol{\tau}) = \prod_{i \in V} \prod_{j=1}^{k_i+1} \mathcal{L}_i(\tau_{i,j-1}, \tau_{i,j}), \quad (4)$$

where

$$\mathcal{L}_i(\tau_{i,j-1}, \tau_{i,j}) = \int L_i(x_{i,\tau_{i,j-1}}, \dots, x_{i,\tau_{i,j}-1} | \theta_{i,j}) \pi_i(\theta_{i,j}) d\theta_{i,j} \quad (5)$$

can be computed. Given a prior for the changepoint parameters,  $\pi(\mathbf{k}, \boldsymbol{\tau})$ , one can consequently compute the posterior density function for the changepoint parameters, up to a normalising constant.

Examples of changepoint models where segment parameters may be marginalised include models for independent and identically distributed data within segments (Fearhead, 2006; Denison et al., 2002), changing linear regressions (Punskaya et al., 2002; Carlin et al., 1992), models for time-dependent data within segments, such as Markov models with time-varying transition matrices (Bolton and Heard, 2018), zero-mean and heteroscedastic processes with changing variance (Johnson et al., 2003), and changepoint models with segment parameters subject to seasonal effects (Turcotte, 2014). Moreover, some model extensions where segment parameters cannot be marginalised, and where segment parameters may be shared across segments, are discussed in Appendix C.2, indicating how the proposed sampling strategy could be adapted for these model extensions.

In particular, consider the class of changepoint models where, within each segment, the data are assumed to be independent and identically distributed such that

$$x_{i,t} \sim f_i(\cdot | \theta_{i,j}), \quad \tau_{i,j-1} \leq t < \tau_{i,j}, \quad (6)$$

for some parametric density  $f_i(\cdot | \theta_{i,j})$  dependent on some segment parameter  $\theta_{i,j} \sim \pi_i(\cdot)$ . The integrals in (5) can be calculated analytically when  $\pi_i$  is chosen to be conjugate to  $f_i$ ; and for non-conjugate cases, (5) may be calculated numerically for low-dimensional segment parameters. For the cyber-security application discussed in Section 2, the changepoint model (6) is suitable for the count data with, for all  $i$ ,  $f_i$  denoting the density of the multinomial distribution with unknown probability parameter vectors  $\theta_{i,j}$  with an uninformative, conjugate prior  $\text{Dirichlet}(\mathbf{1}^M)$ , where  $\mathbf{1}^M$  denotes the  $M$ -dimensional vector of ones. As a result, each changepoint  $\tau_{i,j}$  corresponds to a temporal change in the distribution of counts of logons initiated by the user  $i \in V$  across  $M$  host computers in the network.

### 3.2. Limitations of the standard prior for independent changepoints

When changepoints are assumed to be independent across time series, the posterior distribution of changepoints can be estimated for each time series separately. In this setting, it is standard to assume *a priori* that, for all time series, discrete time changepoints follow a Bernoulli process (Fearhead, 2006) such that

$$\pi(\mathbf{k}, \boldsymbol{\tau} | p) = \prod_{i \in V} p^{k_i} (1-p)^{T-k_i} \mathbb{1}_{\mathcal{T}_i}(\boldsymbol{\tau}_i) \quad (7)$$

for some Bernoulli parameter  $0 < p < 1$ , which encodes prior belief on the expected number of changepoints.

For the cyber-security application where  $G$  represents a network of users, the standard prior in (7) cannot fully encode prior beliefs on changepoints. Appendix A.2 exposes limitations resulting from the assumption of changepoint independence across time series through a comparative study. No choice of  $p$  seems satisfactory: choosing a small value for  $p$  will limit the number of false alerts due to noise in user-specific legitimate activity; yet it will also prevent the detection of weak signals for changes shared by different users which are linked in the network, that may be of great interest. It would be preferable to specify *a priori* that changepoints are more likely to occur simultaneously across time series that are linked in  $G$ , in order to require strong evidence from the data for changes impacting a single user, or possibly weak signals for changes that impact multiple users linked in the network.

## 4. Graphical models for dependent changepoints across multiple time series

This section proposes a novel graphical prior for dependent changepoints across multiple time series. Given the graph of time series  $G = (V, E)$ , where  $V = \{1, \dots, N\}$ , changepoints are modelled by means of an undirected graphical model encoding that pairs of time series  $(i, i') \in E$  are *a priori* likely to be simultaneously affected by changepoints. The graphical model is further extended by relaxing the assumption that dependent changepoints across time series are synchronous; the extended model assumes dependent changepoints across time series correspond to nearby but not necessarily identical time points.

### 4.1. Synchronous dependent changepoints across time series

#### 4.1.1. Model definition

In Section 3.1, changepoints were most simply defined in terms of their number and locations,  $(\mathbf{k}, \boldsymbol{\tau})$ . Subsequently, it will be useful to represent changepoints by means of a binary matrix. For changepoint parameters  $(\mathbf{k}, \boldsymbol{\tau})$ , let  $\mathbf{S} = (S_{i,t})$  be the corresponding binary matrix such that, for all  $i \in V$  and  $t = 1, \dots, T$ ,

$$S_{i,t} = \begin{cases} 1 & \text{if } \exists j \in \{1, \dots, k_i\} \text{ s.t. } t = \tau_{i,j} \\ 0 & \text{otherwise,} \end{cases} \quad (8)$$

so that  $(\mathbf{k}, \boldsymbol{\tau})$  and  $\mathbf{S}$  are equivalent representations of the changepoints. Moreover, let  $S_{i,0} = S_{i,T+1} = 1$  for all  $i$ .

To encode the dependence structure of synchronous changepoints across time series in  $G = (V, E)$ , let  $\boldsymbol{\lambda} = (\lambda_{i,i'})$  be a symmetric matrix of non-negative edge weights for the graph satisfying  $\lambda_{i,i'} > 0$  if and only if  $(i, i') \in E$  for all  $i, i' \in V$ . Then, conditional on  $\boldsymbol{\lambda}$ , changepoints are assumed to have a prior distribution described by the weighted, undirected graph  $G$  such that, for all  $(\mathbf{k}, \boldsymbol{\tau})$ ,

$$\pi(\mathbf{k}, \boldsymbol{\tau} | p, \boldsymbol{\lambda}) = \frac{1}{Z(p, \boldsymbol{\lambda})} \prod_{t=1}^T \exp \left\{ \bar{p} \sum_{i \in V} S_{i,t} + \sum_{i < i'} \lambda_{i,i'} S_{i,t} S_{i',t} \right\}, \quad (9)$$

for some  $0 < p < 1$ , where  $\bar{p} = \text{logit}(p) = \log\{p/(1-p)\}$  and some normalising constant  $Z(p, \boldsymbol{\lambda})$  that has no convenient closed form in general but will present no computational complications since the MCMC algorithm for changepoint parameters proposed in Section 5 only requires computation of ratios of the prior density (9).

If the edge set  $E$  is the empty set, implying  $\lambda_{i,i'} = 0$  for all  $i$  and  $i'$ , then the prior distribution in (9) is equivalent to the standard prior for independent changepoints (7); for all changepoint parameters  $(\mathbf{k}, \boldsymbol{\tau})$  and for all  $0 < p < 1$ ,

$$\pi(\mathbf{k}, \boldsymbol{\tau} | p, \mathbf{0}) = \prod_{i \in V} p^{\sum_{t=1}^T S_{i,t}} (1-p)^{T - \sum_{t=1}^T S_{i,t}}, \quad (10)$$

where  $\mathbf{0}$  is the null matrix. The memoryless property of the standard prior (Fearnhead, 2006) is maintained by the extended prior (9), conditional on fixed value of  $p$ . The latter assumes independent and identical Markov random fields (Lauritzen, 1996) for the columns of  $\mathbf{S}$ . The memoryless property would be lost if (9) were marginalised over a prior distribution for  $p$ .

The graphical prior distribution (9) takes into account both the number of changepoints across time series and their relative positions; the parameter  $p$  controls prior belief on the sparsity of changepoints, and the edge weight parameters  $\boldsymbol{\lambda}$  control the synchronisation of changepoints

between time series. For all pairs  $(i, i')$ , the larger the edge weight  $\lambda_{i,i'} > 0$ , the higher the probability for time series  $i$  and  $i'$  to be simultaneously affected by changepoints. Hence, the prior in (9) may specify changepoints are likely to occur simultaneously across clusters of time series according to  $G$ .

To understand how to set the changepoint prior parameters  $p$  and  $\lambda$  in practice, it is instructive to consider the conditional prior distribution of the components of the binary matrix  $\mathbf{S}$ . Under (9), the conditional distribution of  $S_{i,t}$  given  $\mathbf{S}_{-(i,t)} = \{S_{i',t'} : (i', t') \neq (i, t)\}$  is

$$\pi(S_{i,t} | \mathbf{S}_{-(i,t)}, p, \lambda) \propto \exp \left\{ S_{i,t} \left( \bar{p} + \sum_{i': (i,i') \in E} \lambda_{i,i'} S_{i',t} \right) \right\}, \quad S_{i,t} \in \{0, 1\}. \quad (11)$$

Therefore, for all  $i$  and  $t$ , the hyperparameter  $p$  corresponds to the prior probability that  $t$  is a changepoint for the  $i$ th time series given that no changepoints occur at time  $t$  for the graph neighbour time series of  $i$ ; and, for all  $i'$  such that  $(i, i') \in E$ , the interaction parameter  $\lambda_{i,i'}$  governs how much the conditional prior probability increases if the neighbour time series  $i'$  is impacted by a changepoint at time  $t$ . Moreover, to perceive the influence of the changepoint prior parameters on the posterior distribution of changepoints, it is helpful to consider the full conditional distribution of  $S_{i,t}$  given  $\mathbf{S}_{-(i,t)} = \{S_{i',t'}; (i', t') \neq (i, t)\}$ ,

$$\begin{aligned} \pi(S_{i,t} | \mathbf{S}_{-(i,t)}, p, \lambda, \mathbf{x}) &\propto \left( \frac{\mathcal{L}_i(\tau'_t, t) \mathcal{L}_i(t, \tau''_t)}{\mathcal{L}_i(\tau'_t, \tau''_t)} \right)^{S_{i,t}} \pi(S_{i,t} | \mathbf{S}_{-(i,t)}, p, \lambda) \\ &\propto \exp \left\{ S_{i,t} \left( \log \left\{ \frac{\mathcal{L}_i(\tau'_t, t) \mathcal{L}_i(t, \tau''_t)}{\mathcal{L}_i(\tau'_t, \tau''_t)} \right\} + \bar{p} + \sum_{i': (i,i') \in E} \lambda_{i,i'} S_{i',t} \right) \right\}, \end{aligned} \quad (12)$$

where  $\mathcal{L}_i$  is defined in (5),  $\tau'_t = \max\{t' : t' < t, S_{i,t'} = 1\}$  and  $\tau''_t = \min\{t' : t' > t, S_{i,t'} = 1\}$ . In essence,  $p$  determines the level of evidence required from the data to suggest a changepoint, and the edge weight parameters control, relative to  $p$ , how weak signals for synchronous changepoints can be combined across time series.

#### 4.1.2. A special case: identical edge weight parameters

In practice, it will often be natural to assume that, for all  $(i, i') \in E$ ,  $\lambda_{i,i'} = \lambda$  for some fixed value  $\lambda > 0$ . For all  $i$  and  $t$ , let

$$n_{i,t} = \sum_{i': (i,i') \in E} S_{i',t} \quad (13)$$

be the number of neighbour time series of  $i$  that are affected by a changepoint at time  $t$ . Then, under (9), the conditional prior distribution of  $S_{i,t}$  given  $\mathbf{S}_{-(i,t)} = \{S_{i',t'} : (i', t') \neq (i, t)\}$  is

$$\pi(S_{i,t} | \mathbf{S}_{-(i,t)}, p, \lambda) = \frac{\exp \{S_{i,t} (\bar{p} + \lambda n_{i,t})\}}{\exp \{\bar{p} + \lambda n_{i,t}\} + 1}, \quad S_{i,t} \in \{0, 1\}. \quad (14)$$

Moreover,  $\lambda$  will typically be chosen relative to  $\bar{p}$  and the degree distribution of the nodes in  $G$ . For example, it can be convenient to assume  $\lambda = \lambda_s |\bar{p}| / n$ , where  $n$  denotes the maximum degree of the nodes in  $G$ , for some  $\lambda_s > 0$ .



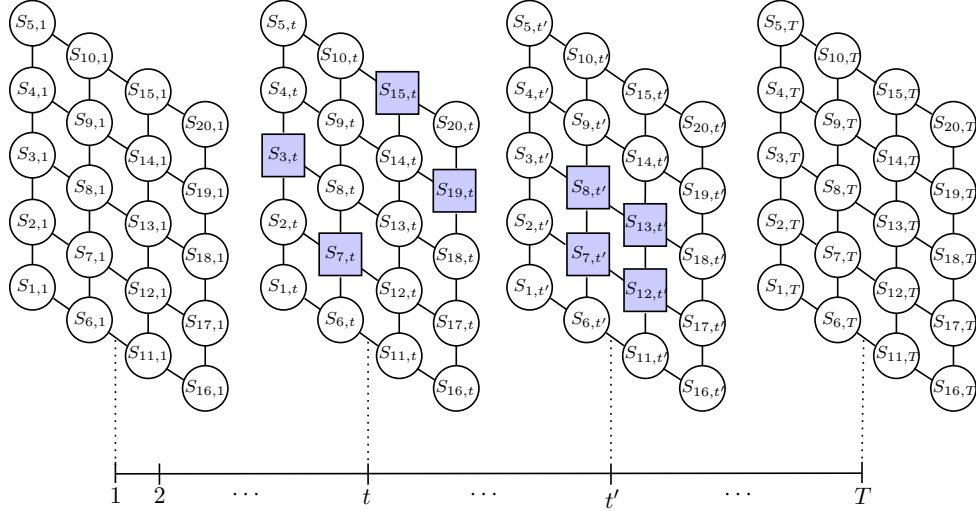


Figure 2: Cartoon representation of a changepoint matrix  $S = (S_{i,t})$ , defined in (8), for 20 time series of length  $T$  which lie on a  $5 \times 4$  lattice graph  $G$ . Edges indicate dependence between components of  $S$  according to the prior (9) given the lattice graph  $G$ . Blue squares indicate  $S_{i,t} = 1$  and white circles indicate  $S_{i,t} = 0$  for all  $i$  and  $t$ .

## 4.2. Examples of graphical dependence structures for changepoints

The prior distribution (9) is suitable for a wide variety of settings. This section provides graph motifs that can be regarded as building blocks to encode the dependence structure of changepoints across multiple time series. For these examples, we assume identical non-zero edge weights as considered in Section 4.1.2 and provide some insight on how to choose the changepoint prior parameters  $p$  and  $\lambda$ . These exemplar dependence structures for changepoints are explored via a simulation study in Appendix D.

### 4.2.1. Lattices

It might be natural to choose the edge set  $E$  to induce an  $N_1 \times N_2$  lattice graph when the number of time series is  $N = N_1 N_2$  for some  $N_1, N_2 > 0$ . For all  $i$ , let  $0 \leq i_1 \leq N_1 - 1$  and  $0 \leq i_2 \leq N_2 - 1$  be the unique natural numbers such that  $i = i_2 N_1 + i_1 + 1$ . Then the  $N_1 \times N_2$  lattice graph is such that  $(i, i') \in E$  if and only if  $|i_1 - i'_1| + |i_2 - i'_2| = 1$ . For example, suppose the data  $x$  are recorded for the analysis of some spatio-temporal phenomenon such that  $x_{i,t}$  denotes the observation at time  $t$  and at the coordinate  $i$  of some  $N_1 \times N_2$  grid over a map of the region of interest, and it is of interest to detect the times and the coordinates at which the distribution of the data changes.

Figure 2 illustrates the dependence structure for changepoints induced by the graphical changepoint prior (9) given a lattice graph  $G$  on 20 time series of length  $T$ . The larger the edge weight  $\lambda > 0$ , the higher the probability for pairs of time series connected on the lattice graph  $G$  to be simultaneously impacted by changepoints. As a result, in Figure 2, changepoints at time  $t'$ , which are connected by edges, are *a priori* more likely than isolated changepoints at time  $t$ . The prior (9) can therefore specify that changepoints are likely to occur as clusters of simultaneous changepoints on the lattice. The conditional probability (14) specifies that  $p$  is the prior probability that a changepoint occurs in isolation on the lattice, and is constrained such that  $n_{i,t} \in \{0, \dots, 4\}$ .

#### 4.2.2. $r$ -chains

Another dependence structure of interest arises when there is a natural ordering of the time series, which is encoded by the time series indices  $1 < \dots < N$ , and changepoints are *a priori* likely to occur as chains of simultaneous changepoints across consecutive time series. For instance, suppose the data consist of multiple time series that are recorded to monitor various aspects of a system; and, it is of interest to detect some event which evolves through multiple phases, such that each phase is likely to manifest through the perturbation of one aspect of the system. In such a setting, it is appropriate to consider the following graph for the time series indices, which we call an  $r$ -chain graph: let  $(i, i') \in E$  if and only if  $1 \leq |i - i'| \leq r$ , for some  $r > 0$  chosen to allow gaps of length  $r - 1$  within chains of changepoints. For  $r$ -chain graphs,  $n_{i,t} \in \{0, \dots, 2r\}$ .

#### 4.2.3. Complete graphs

Suppose a complete graph for the time series indices, that is  $(i, i') \in E$  for all  $i \neq i'$ , so that, according to Section 4.1.2,  $\lambda_{i,i'} = \lambda > 0$  for all  $i \neq i'$ . In such a setting, the prior given in (9) assumes changepoint locations are exchangeable across time series, like the MVCAPA model proposed in Fisch et al. (2022), and therefore solely takes into account the number of time series impacted by a changepoint at time  $t$ , for all  $t$ .

#### 4.2.4. Unknown graph

This article assumes that the graph  $G$  is known *a priori* and contains useful information concerning the dependence structure of changepoints across time series. Future work could reverse this idea and consider applications where estimating  $G$  is one of the inferential objectives. It might often be computationally unrealistic to specify an unconstrained prior for  $G$  admitting that  $\lambda_{i,j} \geq 0$  for all  $(i, i') \in V \times V$ . However, in some settings it might be appropriate to consider a class of possible graphs  $G$ , such as those considered in the previous two subsections; for example, it may be assumed *a priori* that  $G$  is an  $r$ -chain with  $r \geq 0$  unknown.

### 4.3. Extension to asynchronous changepoint dependence

The model in Section 4.1 assumes changepoints are likely to simultaneously affect clusters of time series according to the dependence graph  $G$ . In this section, we relax this model to allow dependence between changepoints in different time series at nearby points in time. The extended model relies on representing changepoints as lagged realisations of simultaneous but unobserved latent changepoints. The latent changepoints are distributed according to the model introduced in Section 4.1 and, conditional on these latent changepoints, time series-specific lags are assumed to be uniformly distributed over some small time window.

Let  $(\mathbf{k}, \boldsymbol{\tau})$  be changepoint parameters for multiple time series as defined in Section 3.1, where it is assumed that the  $i$ th time series is subject to  $k_i$  changepoints whose positions are denoted  $\boldsymbol{\tau}_i = (\tau_{i,1}, \dots, \tau_{i,k_i}) \in \mathcal{T}_{k_i}$  as defined in (3). The asynchronous model further assumes that, for all time series  $i = 1, \dots, N$ , there exist latent changepoint positions  $\tilde{\boldsymbol{\tau}} = (\tilde{\boldsymbol{\tau}}_1, \dots, \tilde{\boldsymbol{\tau}}_N)$ ,  $\tilde{\boldsymbol{\tau}}_i = (\tilde{\tau}_{i,1}, \dots, \tilde{\tau}_{i,k_i}) \in \mathcal{T}_{k_i}$ , and lags  $\mathbf{d} = (\mathbf{d}_1, \dots, \mathbf{d}_N)$ ,  $\mathbf{d}_i = (d_{i,1}, \dots, d_{i,k_i}) \in \{0, \dots, w_i\}^{k_i}$ , for  $\mathbf{w} = (w_1, \dots, w_N)$ , where  $w_i \geq 0$  is an upper bound for the lags, such that, for all  $j = 1, \dots, k_i$ , the  $j$ th changepoint for time series  $i$  is

$$\tau_{i,j} = \tilde{\tau}_{i,j} + d_{i,j}. \quad (15)$$

Let  $\tilde{\tau}_{i,0} = \tau_{i,0} = 0$  and  $\tilde{\tau}_{i,k_i+1} = \tau_{i,k_i+1} = T + 1$ . For all  $(k_i, \boldsymbol{\tau}_i)$  and  $w_i \geq 0$ , if  $\tilde{\boldsymbol{\tau}}_i = \boldsymbol{\tau}_i$  and  $\mathbf{d}_i$  is the zero vector then (15) holds, and therefore the existence of a corresponding pair  $(\tilde{\boldsymbol{\tau}}_i, \mathbf{d}_i)$  with  $\boldsymbol{\tau}_i \in \mathcal{T}_{k_i}$  is guaranteed. If  $w_i = 0$  then the latent changepoints and the changepoints must

be identical; but, in general, given changepoints  $(k_i, \tau_i)$  and  $w_i > 0$ , there are multiple distinct pairs of latent changepoints  $(k_i, \tilde{\tau}_i)$  and lags  $\mathbf{d}_i$  satisfying (15) and  $\tilde{\tau}_i \in \mathcal{T}_{k_i}$ .

For some applications the upper bounds for the lags,  $\mathbf{w}$ , may be fixed. In particular, for some reference time series  $i \in V$ , it can be set that  $w_i = 0$ , implying that  $\tau_{i,j} = \tilde{\tau}_{i,j}$  for all  $j$ , so that changepoints for time series  $i'$  with  $w_{i'} \geq 0$  are lagged relative to changepoints for time series  $i$ . However, in general, upper bounds for the lags will not be known. For example, in the motivational application in cyber-security, no user  $i \in V$  can be assumed to be the first user to be affected by an attack, making it awkward to pick a reference time series  $i$ , and the exact duration of attacks is not known *a priori*. It will be assumed that, independently for all time series  $i$ ,  $w_i \sim \text{Geometric}(\eta)$  for some value  $0 < \eta < 1$  chosen to reflect the expected duration of an attack.

Suppose the latent changepoints  $(\mathbf{k}, \tilde{\tau})$  are distributed according to the prior distribution (9) given some  $0 < p < 1$  and graph edge weight parameters  $\boldsymbol{\lambda}$ . Then, independently for all time series  $i$ , conditional on  $w_i$  and  $(k_i, \tilde{\tau}_i)$ , the lags  $\mathbf{d}_i = (d_{i,1}, \dots, d_{i,k_i})$  are assumed to be uniformly distributed on the set

$$\mathcal{D}(w_i, k_i, \tilde{\tau}_i) = \left\{ (d_{i,1}, \dots, d_{i,k_i}) \in \{0, \dots, w_i\}^{k_i} : (\tilde{\tau}_{i,1} + d_{i,1}, \dots, \tilde{\tau}_{i,k_i} + d_{i,k_i}) \in \mathcal{T}_{k_i} \right\}, \quad (16)$$

such that, for all  $\mathbf{d} = (\mathbf{d}_1, \dots, \mathbf{d}_N)$ ,

$$\pi(\mathbf{d} | \mathbf{k}, \tilde{\tau}, \mathbf{w}) = \prod_{i=1}^N \frac{\mathbb{1}_{\mathcal{D}(w_i, k_i, \tilde{\tau}_i)}(\mathbf{d}_i)}{\text{card}(\mathcal{D}(w_i, k_i, \tilde{\tau}_i))}. \quad (17)$$

Proposition 1 gives a recursion to derive the cardinality of (16).

**Proposition 1.** (Cardinality of  $\mathcal{D}$ ). *Let  $w \geq 0$ ,  $k \geq 0$ ,  $\boldsymbol{\tau} = (\tau_1, \dots, \tau_k) \in \mathcal{T}_k$  with  $\tau_0 = 1$  and  $\tau_{k+1} = T + 1$ , and let  $\mathcal{D}(w, k, \boldsymbol{\tau})$  be the set defined in (16).*

(i) *For all  $j \geq 1$  and  $l \geq 0$ , let  $\rho(j, l) = \min\{w + 1, T + 1 - \tau_j\} - (\tau_{j+l} - \tau_j)$  and*

$$Q(j, l) = \frac{(\rho(j, l) + l)!}{(\rho(j, l) - 1)!(l + 1)!} \mathbb{1}_{\{0, \dots, w\}}(\tau_{j+l} - \tau_j). \quad (18)$$

*Additionally, let  $Z(0) = 1$ ,  $Z(1) = Q(1, 0)$  and, recursively for all  $k > 1$ ,*

$$Z(k) = \sum_{j=1}^k (-1)^{k-j} Z(j-1) Q(j, k-j). \quad (19)$$

*Then*

$$\text{card}(\mathcal{D}(w, k, \boldsymbol{\tau})) = Z(k). \quad (20)$$

*In particular, if  $k = 0$  then  $\boldsymbol{\tau}$  is the empty sequence and  $\mathcal{D}(w, k, \boldsymbol{\tau})$  contains a unique element, namely the empty sequence.*

(ii)  *$\text{card}(\mathcal{D}(w, k, \boldsymbol{\tau})) \leq (w + 1)^k$  and the equality holds if and only if  $\tau_{j+1} - \tau_j > w$  for all  $j$ .*

*Proof.* See Appendix B. □

Consequently, the joint prior density for  $(\mathbf{k}, \tilde{\tau}, \mathbf{d})$  is

$$\pi(\mathbf{k}, \tilde{\tau}, \mathbf{d} | p, \boldsymbol{\lambda}, \mathbf{w}) = \frac{\pi(\mathbf{k}, \tilde{\tau} | p, \boldsymbol{\lambda})}{\prod_{i=1}^N \text{card}(\mathcal{D}(w_i, k_i, \boldsymbol{\tau}_i))} \quad (21)$$

and the induced changepoint prior distribution for  $(\mathbf{k}, \boldsymbol{\tau})$  is

$$\pi(\mathbf{k}, \boldsymbol{\tau} | p, \boldsymbol{\lambda}, \mathbf{w}) = \sum_{(\tilde{\boldsymbol{\tau}}, \mathbf{d}) \in \Upsilon(\mathbf{k}, \boldsymbol{\tau}, \mathbf{w})} \pi(\mathbf{k}, \tilde{\boldsymbol{\tau}}, \mathbf{d} | p, \boldsymbol{\lambda}, \mathbf{w}), \quad (22)$$

where  $\Upsilon(\mathbf{k}, \boldsymbol{\tau}, \mathbf{w})$  denotes the set of pairs of latent changepoints and lags,  $(\mathbf{k}, \tilde{\boldsymbol{\tau}}, \mathbf{d})$ , that identify the changepoints  $(\mathbf{k}, \boldsymbol{\tau})$  according to (15).

## 5. Markov chain Monte Carlo inference

Joint sampling of changepoints across time series is required when the assumption of independence for changepoints is relaxed. In this section, we propose a reversible jump MCMC algorithm (Green, 1995) to sample changepoints in multiple time series,  $(\mathbf{k}, \boldsymbol{\tau})$ . The changepoint parameter space is augmented with auxiliary variables (Besag and Green, 1993; Higdon, 1998) that induce clusters of time series indices according to  $G$ . Then, the reversible jump MCMC algorithm of Denison et al. (2002) is extended to sample from the augmented parameter space, thereby providing a means to efficiently explore the changepoint parameter space. At each iteration of the algorithm, a new cluster of changepoints may be proposed or an existing cluster of changepoints may be deleted or shifted. The validity of the proposed MCMC algorithm follows immediately from the reversibility of the proposed moves. Appendix C gives some indications on the time complexity of the algorithm and discusses possible extensions for settings where segment parameters cannot be marginalised. For notational simplicity it is assumed there are no missing data, but even with data which are not independent and identically distributed within segments, any missing observations would present no methodological complication, since missing data can be sampled from their predictive distribution within the proposed MCMC scheme (Gelman et al., 2004).

### 5.1. Sampler for synchronous dependent changepoints

We begin by proposing an MCMC algorithm to sample from the posterior distribution of changepoints when changepoint parameters are *a priori* distributed according to the prior introduced in Section 4.1,  $\pi(\mathbf{k}, \boldsymbol{\tau} | p, \boldsymbol{\lambda})$ , given  $0 < p < 1$  and some interaction parameters  $\boldsymbol{\lambda}$ .

To sample changepoints for multiple time series, consider the following adaptation of the standard MCMC algorithm to sample changepoints for a unique time series (Denison et al., 2002), which will be called the “single site updating” MCMC algorithm thereafter. At each iteration of the algorithm, with  $(\mathbf{k}, \boldsymbol{\tau})$  denoting the latest particle of the sample chain, propose one of the following two moves: for a uniformly chosen index  $(i, t)$ , propose  $S_{i,t}$  to be updated to  $1 - S_{i,t}$ , thereby allowing birth or death of a changepoint; alternatively, the position of a randomly chosen changepoint,  $\tau_{i,j}$ , is sampled uniformly from  $\{\tau_{i,j-1} + 1, \dots, \tau_{i,j+1} - 1\}$ .

With the graphical prior distribution (9), synchronous changepoints can be correlated across time series, and the single site updating MCMC algorithm can become impractical, as illustrated in Appendix D.4.3 through a simulation study. Instead, it will be necessary to propose moves that allow birth, death or shift of clusters of synchronous changepoints according to the graph induced by  $\boldsymbol{\lambda}$ .

#### 5.1.1. Augmenting the parameter space with auxiliary variables

To provide a means of moving efficiently through the state space of the changepoint parameters, the parameter space is augmented with binary auxiliary variables  $\mathbf{u} = (\mathbf{u}_1, \dots, \mathbf{u}_T)$  such that, for all  $t$ ,  $\mathbf{u}_t$  is an  $N \times N$  symmetric binary graph adjacency matrix with  $(i, i')$  element  $u_t(i, i')$ .

For all  $t$ , the prior density of  $\mathbf{u}_t$  is assumed to take the conditionally independent form

$$\pi(\mathbf{u}_t | \boldsymbol{\lambda}, \delta, \mathbf{k}, \boldsymbol{\tau}) = \prod_{i < i'} q_t(i, i')^{u_t(i, i')} \{1 - q_t(i, i')\}^{1 - u_t(i, i')}, \quad (23)$$

where

$$q_t(i, i') = 1 - \exp\{-\delta \lambda_{i, i'} (1 - |S_{i, t} - S_{i', t}|)\} \quad (24)$$

is the conditional probability that  $u_t(i, i') = 1$ , given a partial decoupling parameter  $\delta \geq 0$  (Higdon, 1998) whose role will be discussed in Section 5.1.2. After observing data  $\mathbf{x}$  distributed according to (6), the joint posterior density of the augmented parameters  $(\mathbf{k}, \boldsymbol{\tau}, \mathbf{u})$  is

$$\pi(\mathbf{k}, \boldsymbol{\tau}, \mathbf{u} | p, \boldsymbol{\lambda}, \mathbf{x}, \delta) = \pi(\mathbf{u} | \boldsymbol{\lambda}, \delta, \mathbf{k}, \boldsymbol{\tau}) \pi(\mathbf{k}, \boldsymbol{\tau} | p, \boldsymbol{\lambda}, \mathbf{x}), \quad (25)$$

where

$$\pi(\mathbf{u} | \boldsymbol{\lambda}, \delta, \mathbf{k}, \boldsymbol{\tau}) = \prod_{t=1}^T \pi(\mathbf{u}_t | \boldsymbol{\lambda}, \delta, \mathbf{k}, \boldsymbol{\tau}). \quad (26)$$

For all  $t$ , consider the graph  $H_t = (V, E_t)$  with vertex set  $V = \{1, \dots, N\}$  and edge set  $E_t$  such that  $(i, i') \in E_t$  if and only if  $u_t(i, i') = 1$  for all  $i, i' \in V$ . According to (24), if  $u_t(i, i') = 1$  then  $q_t(i, i') > 0$  and, consequently,  $S_{i, t} = S_{i', t}$ . As a result, with  $\mathcal{C}_t$  denoting the set of connected components of  $H_t$ , for all clusters of time series  $\gamma \in \mathcal{C}_t$ ,  $S_{i, t} = S_{i', t}$  for all  $i, i' \in \gamma$ . In other words, the auxiliary variables  $\mathbf{u}_t$  induce a partition of the time series,  $\mathcal{C}_t$ , such that, for each cluster  $\gamma \in \mathcal{C}_t$ , either all time series or no time series in  $\gamma$  are affected by a changepoint at time  $t$ . Moreover, according to (24), if  $S_{i, t} = S_{i', t}$  then the conditional probability that  $u_t(i, i') = 1$  increases with  $\lambda_{i, i'} > 0$ , so that clusters induced by  $\mathbf{u}_t$  will tend to be clusters on the graph induced by the edge weight parameters.

### 5.1.2. MCMC algorithm

To generate realisations from the posterior distribution of the changepoints, we consider a ‘‘cluster updating’’ MCMC algorithm that samples from the extended joint posterior density (25). By inducing clusters of time series determined by the edge weight parameters for each time point  $t$ , the auxiliary variables  $\mathbf{u}$  provide a means to efficiently explore the state space of  $(\mathbf{k}, \boldsymbol{\tau})$ .

The parameter  $\delta$  is a tuning parameter for the cluster updating MCMC algorithm. The size of clusters will tend to increase with  $\delta$ ; in particular, if  $\delta = 0$  then, for all  $t$ , each cluster corresponds to a unique time series index, even if the edge weights of the dependence graph are large, so that the ‘‘cluster updating’’ MCMC algorithm reduces to the ‘‘single site updating’’ algorithm. Typically  $\delta$  is fixed (Higdon, 1998) to control the probabilities in (23) and therefore the expected size of clusters. However, we propose to treat  $\delta \geq 0$  as an unknown parameter with prior distribution  $\pi(\delta)$ , so that expected sizes of cluster may vary in the sample; specifically, we assume that  $\delta = 0$  with probability  $0 \leq \delta_0 \leq 1$  and otherwise  $\delta$  is drawn from Beta( $\delta_1, \delta_2$ ) for  $\delta_1, \delta_2 > 0$ .

For the cluster updating MCMC algorithm, at each iteration of the algorithm, with  $(\mathbf{k}, \boldsymbol{\tau}, \mathbf{u}, \delta)$  denoting the latest particle of the sample chain, one of the following moves is proposed.

#### Birth/death move

Conditional on the auxiliary variables, the birth/death move proposes the birth or death of a cluster of synchronous changepoints. Sample  $t'$  uniformly from  $\{1, \dots, T\}$ . A cluster  $\gamma$  of time series indices is randomly chosen from  $\mathcal{C}_{t'}$ , the set of clusters of time series induced by the auxiliary

variables  $\mathbf{u}_{t'}$ . Then, leaving the auxiliary variables unchanged, propose changepoint parameters  $(\mathbf{k}', \boldsymbol{\tau}')$  such that, for all  $i = 1, \dots, N$  and  $t = 1, \dots, T$ ,

$$S'_{i,t} = \begin{cases} 1 - S_{i,t} & \text{if } i \in \gamma \text{ and } t = t' \\ S_{i,t} & \text{otherwise,} \end{cases} \quad (27)$$

where  $\mathbf{S}$  and  $\mathbf{S}'$  are binary matrix representations of  $(\mathbf{k}, \boldsymbol{\tau})$  and  $(\mathbf{k}', \boldsymbol{\tau}')$  according to (8), respectively.

### Shift move

The shift move proposes to shift the position of a cluster of synchronous changepoints. First, a time unit  $t$  is uniformly chosen from  $\{t : \sum_{i=1}^N S_{i,t} > 0\}$ . Let  $\mathcal{C}_t^* \subseteq \mathcal{C}_t$  denote the set of clusters of time series indices  $\gamma$  induced by  $\mathbf{u}_t$  such that, for all  $i \in \gamma$ ,  $S_{i,t} = 1$ . A cluster  $\gamma$  is uniformly chosen from  $\mathcal{C}_t^*$ . For all  $i \in \gamma$ , let  $j_i$  be the index of the changepoint with position  $t$  for the  $i$ th time series, that is  $\tau_{i,j_i} = t$ . Then, sample uniformly  $t'$  from  $\bigcap_{i \in \gamma} \{\tau_{i,j_i-1} + 1, \dots, \tau_{i,j_i+1} - 1\}$  and propose changepoint parameters  $(\mathbf{k}, \boldsymbol{\tau}')$  that are identical to  $(\mathbf{k}, \boldsymbol{\tau})$  but with  $\tau'_{i,j_i} = t'$ , for all  $i \in \gamma$ .

In parallel, it is required to propose auxiliary variables  $\mathbf{u}'$  which are adapted to  $(\mathbf{k}, \boldsymbol{\tau}')$ . The updated auxiliary variables differ from  $\mathbf{u}$  as follows. For all  $i, i' \in \gamma$ ,  $u'_{t'}(i, i') = u_t(i, i')$  and  $u'_t(i, i') = u_{t'}(i, i')$ ; for all  $i \in \gamma$  and  $i' \notin \gamma$  such that  $t' \notin \boldsymbol{\tau}_{i'}$ ,  $u'_{t'}(i, i') = 0$ ; and, ensuring reversibility of the move, for all  $i \in \gamma$  and  $i' \notin \gamma$  such that  $t \notin \boldsymbol{\tau}_{i'}$ ,  $u'_t(i, i')$  is sampled conditionally on  $(\mathbf{k}, \boldsymbol{\tau}')$  according to the Bernoulli  $(1 - \exp\{-\delta \lambda_{i,i'}(1 - |S_{i,t} - S'_{i,t}|\})$  target distribution implied by (23).

### Update of auxiliary variables

Changepoints are left unchanged,  $\delta$  is sampled from its prior distribution, and auxiliary variables are sampled from the full conditional distribution given in (23), thereby proposing an updated clustering of time series indices for all  $t$ .

## 5.2. Sampler for asynchronous dependent changepoints

According to the changepoint model (22) introduced in Section 4.3, changepoints do not need to occur at the same time to be related. Consequently, to explore the changepoint parameter space it will be required to propose the birth, death or shift of clusters of asynchronous changepoints. This section extends the MCMC algorithm from Section 5.1 to sample from the posterior distribution of changepoints when changepoint parameters are *a priori* distributed according to  $\pi(\mathbf{k}, \boldsymbol{\tau} | p, \boldsymbol{\lambda}, \boldsymbol{w})$  from (22).

Recall that under the asynchronous model, changepoints  $(\mathbf{k}, \boldsymbol{\tau})$  are deterministically specified by latent changepoints  $(\mathbf{k}, \tilde{\boldsymbol{\tau}})$  and unknown lags  $\mathbf{d}$  according to (15). Therefore, a sample from  $(\mathbf{k}, \boldsymbol{\tau})$  can be obtained from a sample from  $(\mathbf{k}, \tilde{\boldsymbol{\tau}}, \mathbf{d})$ . Next, we propose a sampler from the joint posterior distribution of  $(\mathbf{k}, \tilde{\boldsymbol{\tau}}, \mathbf{d})$ , updated from the prior density (21) by the observed data  $\mathbf{x}$ , thereby providing a means to obtain a sample from the posterior distribution of  $(\mathbf{k}, \boldsymbol{\tau})$ .

As in Section 5.1, the parameter space is augmented with auxiliary variables  $\mathbf{u} = (\mathbf{u}_1, \dots, \mathbf{u}_T)$  to facilitate the exploration of the state space of the parameters of interest  $(\mathbf{k}, \tilde{\boldsymbol{\tau}}, \mathbf{d})$ . Conditionally on latent changepoints  $(\mathbf{k}, \tilde{\boldsymbol{\tau}})$  and independently of the lags and the data, for all  $t$  and  $i < i'$ ,  $u_t(i, i')$  is assumed to be distributed according to (23), such that  $u_t(i, i') \sim \text{Bernoulli}\left(1 - \exp\{-\delta \lambda_{i,i'}(1 - |\tilde{S}_{i,t} - \tilde{S}'_{i',t}|\})\right)$ , where  $\tilde{\mathbf{S}}$  is the binary matrix representation of  $(\mathbf{k}, \tilde{\boldsymbol{\tau}})$  according to (8). As described in Section 5.1.1, it follows that the auxiliary variables  $\mathbf{u}_t$  induce a partition of the time series,  $\mathcal{C}_t$ , such that, for each cluster  $\gamma \in \mathcal{C}_t$ , either all time series or no time series in  $\gamma$  are affected by a latent changepoint at time  $t$ .

The joint posterior density of the augmented parameters  $(\mathbf{k}, \tilde{\boldsymbol{\tau}}, \mathbf{d}, \mathbf{u})$  is

$$\pi(\mathbf{k}, \tilde{\boldsymbol{\tau}}, \mathbf{d}, \mathbf{u} | p, \boldsymbol{\lambda}, \mathbf{w}, \mathbf{x}, \delta) = \pi(\mathbf{u} | \boldsymbol{\lambda}, \delta, \mathbf{k}, \tilde{\boldsymbol{\tau}}) \pi(\mathbf{k}, \tilde{\boldsymbol{\tau}}, \mathbf{d} | p, \boldsymbol{\lambda}, \mathbf{w}, \mathbf{x}). \quad (28)$$

To sample from the posterior distribution of  $(\mathbf{k}, \tilde{\boldsymbol{\tau}}, \mathbf{d}, \mathbf{u})$ , or  $(\mathbf{k}, \tilde{\boldsymbol{\tau}}, \mathbf{d}, \mathbf{u}, \mathbf{w})$  if upper bounds for the lags are *a priori* unknown, the MCMC algorithm discussed in Section 5.1 is extended as follows: the birth/death and shift moves are adapted to pairs of latent changepoints and lags; and additional moves are introduced for updating the lags. For the lags, note that according to (16), for all  $i = 1, \dots, N$  and  $j = 1, \dots, k_i$ , to maintain monotonicity in the changepoints, the lag associated to the  $j$ th changepoint of the  $i$ th time series must satisfy

$$d_{i,j} \in \mathcal{D}_j(w_i, k_i, \tilde{\boldsymbol{\tau}}_i) = \{\ell \in \mathbb{N}; d_- \leq \ell \leq d^+\}, \quad (29)$$

where  $d_- = \max(0, d_{i,j-1} + \tau_{i,j-i} - \tau_{i,j} + 1)$  and  $d^+ = \min(w_i, d_{i,j+1} + \tau_{i,j+1} - \tau_{i,j} - 1)$ ; and the full conditional probability distribution of  $d_{i,j}$  is such that, for all  $d_{i,j} \in \mathcal{D}_j(w_i, k_i, \tilde{\boldsymbol{\tau}}_i)$ ,

$$\pi(d_{i,j} | \mathbf{d}_{-(i,j)}, k_i, \tilde{\boldsymbol{\tau}}_i, w_i, \mathbf{x}_i) \propto \mathcal{L}_i(\tilde{\tau}_{i,j-1} + d_{i,j-1}, \tilde{\tau}_{i,j} + d_{i,j}) \mathcal{L}_i(\tilde{\tau}_{i,j} + d_{i,j}, \tilde{\tau}_{i,j+1} + d_{i,j+1}) \quad (30)$$

where  $\mathbf{d}_{-(i,j)} = \{d_{i',j'}; (i', j') \neq (i, j)\}$  and  $\mathcal{L}_i$  is defined in (5).

For the extended cluster updating MCMC algorithm, at each iteration of the algorithm, with  $(\mathbf{k}, \tilde{\boldsymbol{\tau}}, \mathbf{d}, \mathbf{u}, \mathbf{w})$  denoting the latest particle of the sample chain, one of the following moves is proposed.

### Extended birth/death move

The extended birth/death move proposes the birth or death of a cluster of asynchronous changepoints. First, conditionally on the auxiliary variables, latent changepoints  $(\mathbf{k}', \tilde{\boldsymbol{\tau}}')$  are proposed according to the birth/death move detailed in Section 5.1: for all time series  $i \in \gamma \subseteq \{1, \dots, N\}$ , the birth or death of latent changepoint with position  $t$  is proposed. Then, updated lags are proposed conditional on  $(\mathbf{k}', \tilde{\boldsymbol{\tau}}')$ : If the birth of changepoints is proposed, then, for all time series  $i \in \gamma$ , there is  $j_i$  such that  $\tilde{\tau}'_{i,j_i} = t$ , and the lags  $\mathbf{d}'_i = (d_{i,1}, \dots, d_{i,j_i-1}, d'_{i,j_i}, d_{i,j_i+1}, \dots, d_{i,k_i})$  are proposed for the  $i$ th time series, where  $d'_{i,j_i}$  is sampled from the full conditional distribution (30); otherwise, if the death of changepoints is proposed, then, for all  $i \in \gamma$ , there is  $j_i$  such that  $\tilde{\tau}_{i,j_i} = t$ , and the lags  $\mathbf{d}'_i = (d_{i,1}, \dots, d_{i,j_i-1}, d_{i,j_i+1}, \dots, d_{i,k_i})$  are proposed for the  $i$ th time series.

### Extended shift move

The extended shift move proposes to shift the positions of a cluster of asynchronous changepoints. First, latent changepoints  $(\mathbf{k}', \tilde{\boldsymbol{\tau}}')$  and auxiliary variables  $\mathbf{u}'$  are proposed according to the shift move discussed in Section 5.1: for all time series with index  $i \in \gamma$ , the position  $t'$  is proposed for latent changepoint with position  $t$ . Then, for all  $i \in \gamma$ , letting  $j_i$  denote the index such that  $\tilde{\tau}'_{i,j_i} = t'$ , propose  $d'_{i,j_i}$  from the full conditional distribution (30).

### Update of auxiliary variables

$\delta$  is sampled from its prior distribution and, conditional on latent changepoints  $(\mathbf{k}, \tilde{\boldsymbol{\tau}})$ , auxiliary variables are sampled from their full conditional distribution (23).

### Update of lags

A pair  $(i, j)$  is uniformly chosen from  $\{(i, j); i = 1, \dots, N \text{ and } j = 1, \dots, k_i\}$ , and the lag  $d_{i,j}$  is sampled from the full conditional distribution given in (30).

## Update of upper bounds for lags

If the maximal lags  $w$  are *a priori* unknown, for a randomly chosen time series with index  $i$  it is proposed to update  $w_i$  to  $w'_i = w_i + \sigma$  with probability  $1/2$ , and to update  $w_i$  to  $w'_i = |w_i - \sigma|$  otherwise, where  $\sigma$  is drawn from  $\text{Geometric}(\rho)$  for some  $0 < \rho < 1$ . Proposing to update  $w_i$  requires proposing updated lags  $\mathbf{d}'_i = (d'_{i,1}, \dots, d'_{i,k_i}) \in \mathcal{D}(w'_i, k_i, \tilde{\tau}_i)$  for the  $i$ th time series. For  $j = 1, \dots, k_i$ , given  $w'_i$  and  $(d'_{i,1}, \dots, d'_{i,j-1}, d_{i,j+1}, \dots, d_{i,k_i})$ , the lag  $d'_{i,j}$  is sampled from the full conditional distribution (30).

## 6. Estimating changepoint parameters

To summarise the posterior distribution of changepoint parameters for multiple time series, for each time series  $i$ , following Green (1995), one may consider the posterior marginal distribution of the number of changepoints  $k_i$ , and the posterior distribution of the changepoint positions  $\tau_i$  conditional on  $k_i$ . However, in practice, for each time series  $i$ , it may be necessary to report a point estimate  $(\hat{k}_i, \hat{\tau}_i)$  for the changepoint parameters  $(k_i, \tau_i)$ . Following normative Bayesian theory, to define an optimal Bayes estimate for changepoints, we propose a loss function that evaluates the quality of estimated changepoints. When assessing the cost associated with the estimate  $(\hat{k}_i, \hat{\tau}_i)$  of  $(k_i, \tau_i)$ , both the number and the positions of changepoints must be taken into account. To address this challenge, we use matchings in graphs, as defined in Definition 1 and Definition 2, to define a loss function  $L$  for changepoint estimates in Definition 3.

**Definition 1.** (Maximum matching in a graph). *Let  $B = (V, E)$  be a graph where  $V$  is a vertex set and  $E \subseteq V \times V$  is an edge set. A matching  $M$  in  $B$  is a subset of  $E$  such that no two edges in  $M$  share a common vertex. A maximum matching in  $B$  is a matching that is not a subset of a larger matching in  $B$ .*

**Definition 2.** (Minimum weight maximum matching in a graph). *Let  $B = (V, E)$  be a graph with weights  $w_{i,j} \geq 0$  for all  $(i, j) \in E$ . A minimum weight maximum matching in  $B$  is a maximum matching in  $B$  for which the sum of weights of the edges is minimised.*

When  $B$  is a weighted bipartite graph, the Kuhn–Munkres algorithm, also known as the Hungarian algorithm, (Bondy and Murty, 1976) finds a minimum weight maximum matching in  $B$ ; the time complexity of the algorithm is  $\mathcal{O}(\text{card}(E)\text{card}(V) + \text{card}(V)^2 \log \log \text{card}(V))$ , where  $\text{card}(V)$  and  $\text{card}(E)$  denote the cardinality of the vertex set and the cardinality of the edge set of  $B$ , respectively.

**Definition 3.** (Loss function  $L$  for changepoint estimates). *Let  $\gamma \geq 0$ . For all  $k_i, \hat{k}_i \geq 0$ ,  $\tau_i = (\tau_{i,1}, \dots, \tau_{i,k_i}) \in \mathcal{T}_{k_i}$  and  $\hat{\tau}_i = (\hat{\tau}_{i,1}, \dots, \hat{\tau}_{i,\hat{k}_i}) \in \mathcal{T}_{\hat{k}_i}$  (3), let  $B_i$  be the weighted complete bipartite graph with vertex sets  $V_i = \{0, \dots, k_i\}$  and  $\hat{V}_i = \{0, \dots, \hat{k}_i\}$ , and weights*

$$w_{i,j,j'} = \min\{\gamma, |\tau_{i,j} - \hat{\tau}_{i,j'}|\} \quad (31)$$

for all  $j \in V_i$  and  $j' \in \hat{V}_i$ . Given a minimum weight maximum matching  $M_i$  in  $B_i$ , for all  $j \in V_i$  and  $j' \in \hat{V}_i$ , let  $m_{i,j,j'} = 1$  if  $j$  and  $j'$  are matched, that is  $(j, j') \in M_i$ , and  $m_{i,j,j'} = 0$  otherwise. Then, define the loss to be

$$L \left[ (\hat{k}_i, \hat{\tau}_i), (k_i, \tau_i) \right] = \gamma |\hat{k}_i - k_i| + \frac{1}{2} \sum_{j \in V_i} \sum_{j' \in \hat{V}_i} m_{i,j,j'} w_{i,j,j'}. \quad (32)$$

Consider the complete bipartite graph  $B_i$  with independent vertex sets  $V_i = \{0, \dots, k_i\}$ ,  $\hat{V}_i = \{0, \dots, \hat{k}_i\}$  and weights (31). A minimum weight maximum matching  $M_i$  in  $B_i$  gives a matching of the elements of  $\hat{\tau}_i$  and  $\tau_i$  that minimises the sum of distances (31) between



matched changepoints. Given  $M_i$ , according to the loss function (32), the cost associated with the estimate  $(\hat{k}_i, \hat{\tau}_i)$  of  $(k_i, \tau_i)$  is then obtained by adding the cost  $\gamma$  for each unmatched changepoint and the total distance between matched changepoints. Note that according to (31), the cost of matching two changepoint positions, that are separated by more than  $\gamma$  time units, is equal to the cost of an unmatched changepoint, namely  $\gamma$ . Therefore, the loss function  $L$  takes into account both the number and the positions of changepoints, and the cost  $\gamma$  is chosen to be the maximum acceptable distance between a changepoint position and its estimated position. The optimal Bayes estimate  $(\hat{k}_i, \hat{\tau}_i)$  is the changepoint parameters that minimise the expected posterior loss with respect to the posterior marginal distribution of the changepoints  $(k_i, \tau_i)$ .

Given an approximate sample from the posterior distribution (Section 5), an approximate Bayes estimate  $(\hat{k}_i, \hat{\tau}_i)$  for each series can be identified numerically by finding within the sample the changepoint parameters that minimise the estimated posterior expected loss.

Appendix D presents a simulation study that demonstrates the model introduced in Section 4 and the MCMC sampling strategy discussed in Section 5, using the loss function introduced in this section. In particular, various graphs and changepoint parameters are considered to illustrate the flexibility of the proposed model, and the convergence of the sampler is demonstrated under a wide range of settings.

## 7. Red team detection in network authentication data from LANL

This section presents results of an analysis of the LANL network authentication data presented in Section 2 that demonstrates the utility of the graphical changepoint model proposed in Section 4.

### 7.1. Presence of a red team

The occurrence of a red team exercise during the first month of the data collection provides surrogate intruder behaviour in the authentication data (Kent, 2015). In particular, 103 user IDs are known to have been used by the red team. We show the graphical model for dependent changepoints can combine evidence from multiple users which are linked in the network, to detect chains of quasi-synchronous weak signals for changes in the authentication activity of red team users, whilst limiting the number of false alerts.

For our demonstration purposes, it suffices to examine a subset of the full LANL network of users, which is represented by the graph  $G = (V, E)$  defined in Section 2.2. Let  $R$  denote the set of red team users and let  $B \subseteq \{u \in V \setminus R : \exists r \in R \text{ s.t. } (u, r) \in E\}$  denote  $\text{card}(R)$  randomly selected users that are not labelled as red team users in the data but are linked to red team users on the network. The focus is on the network corresponding to the subgraph  $G'$  induced in  $G$  by the set of users  $V' = R \cup B$ . Figure 3 shows the degree distribution of the 206 users in  $G'$ . Red team users tend to have a greater degree in  $G'$  than legitimate users; to traverse the network towards high value targets, intruders tend to take control of users that are highly linked on the network.

### 7.2. Changepoint modelling

Recall from Section 2 that, for each user  $i \in V'$ , the data  $x_{i,0}, \dots, x_{i,T}$  consist of hourly counts of network logons per source computer for the first month of data collection as defined in (2), which are now assumed to follow the model specified in (6) for multinomial data. Different graphical changepoint priors are considered to demonstrate the benefits of encoding prior beliefs about cyber-attacks. To encode prior belief that signals for changes resulting from an attack are likely to occur at similar times across users that are linked in the network  $G'$ , the graphical changepoint prior specified in (22) is considered with an identical edge weight parameter  $\lambda > 0$ ,

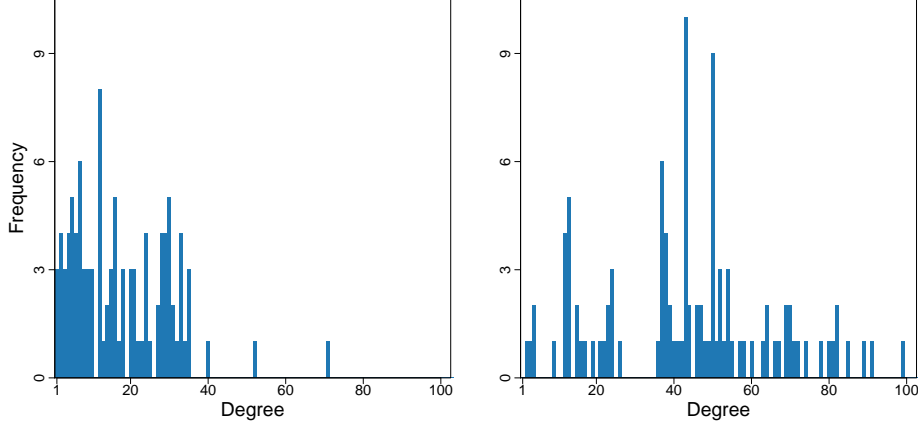


Figure 3: Degree distribution of users in the LANL network represented by the graph  $G'$ . Left panel: counts for legitimate users. Right panel: counts for red team users.

as defined in Section 4.1.2, for all pairs of time series corresponding to users that are linked in  $G'$ . Moreover, for comparison purposes, the graphical changepoint prior (22) is also considered assuming the complete graph defined in Section 4.2.3 such that  $\lambda_{i,j} = \lambda > 0$  for all pairs of users  $(i, j) \in V' \times V'$ . With  $\lambda = 0$ , the two graphical changepoint priors of interest correspond to the standard changepoint model assuming independence of changepoints across time series (10).

For comparison purposes and to illustrate the flexibility of the proposed model, a collection of changepoint prior parameters are considered:  $\bar{p} \in \{-30, -50, -70\}$  and  $\lambda = \lambda_s |\bar{p}|/n$  with  $\lambda_s \in \{0, 0.5, 0.6, 0.7, 0.8\}$ , where  $n$  denotes the average node degree in the graph. Moreover, different assumptions for the upper bounds  $w$  for the lags are compared: the *zero window* assumption with  $w_i = 0$  for all  $i$ , implying signals for attacks are assumed to be synchronous across users; and, the *variable window* assumption with  $w_i \sim \text{Geometric}(0.9)$  for all  $i$ , admitting signals for attacks may be asynchronous across users.

For each simulation, a sample of size 1 000 000 was obtained from the posterior distribution of the changepoints via the MCMC algorithm proposed in Section 5.2, with a burn-in of 300 000 iterations; the Bayes estimate for changepoints corresponding to the loss function (32) with  $\gamma = 48$  was then derived from the sample.

### 7.3. Results

For each user in the network, each estimated changepoint represents a piece of evidence for possible malicious behaviour that might require further investigation by cyber analysts. Identifying inferred changepoints for time series corresponding to legitimate users  $i \in B$  as false alerts, it is meaningful to compare models in terms of the estimated number of changepoints per time series  $i \in V'$ ,

$$\bar{k} = \frac{1}{\text{card}(V')} \sum_{i \in V'} k_i, \quad (33)$$

and the proportion of estimated changepoints that impact redteam users,

$$k^{R/V'} = \frac{\sum_{i \in R} k_i}{\sum_{i \in V'} k_i}. \quad (34)$$

Moreover, since cyber-attacks tend to be identified through clusters of behavioural changes across machines that are linked on the network, it is of interest to prioritise for investigation the estimated

change points that belong to clusters of quasi-synchronous change points on the network. Given some time window  $\varpi \geq 0$ , let the weight of  $\tau_{i,j}$  be

$$c_{i,j}^{\varpi} = \frac{n_{i,j}^{\varpi} + 1}{n_i + 1}, \quad (35)$$

where

$$n_{i,j}^{\varpi} = \text{card}(\{(i, i') \in E : \exists j' \in \{1, \dots, k_{i'}\} \text{ s.t. } |\tau_{i,j} - \tau_{i',j'}| \leq \varpi\}) \quad (36)$$

denote the number of users linked to user  $i$  in  $G'$  that are impacted by a change point within  $\varpi$  hours of  $\tau_{i,j}$ , and where  $n_i = \text{card}(\{(i, i') \in E\})$  is the degree of node  $i$  in  $G'$ , such that  $(n_i + 1)^{-1} \leq c_{i,j} \leq 1$ . The larger the weight  $c_{i,j}$ , the more connected  $\tau_{i,j}$  to other change points across the network. To take into account both the number of change points and their connectedness, for each user  $i$ , change point estimates are also compared via the sum of weights

$$m_i \equiv m_i^{\varpi} = \sum_{j=1}^{k_i} c_{i,j}^{\varpi}, \quad (37)$$

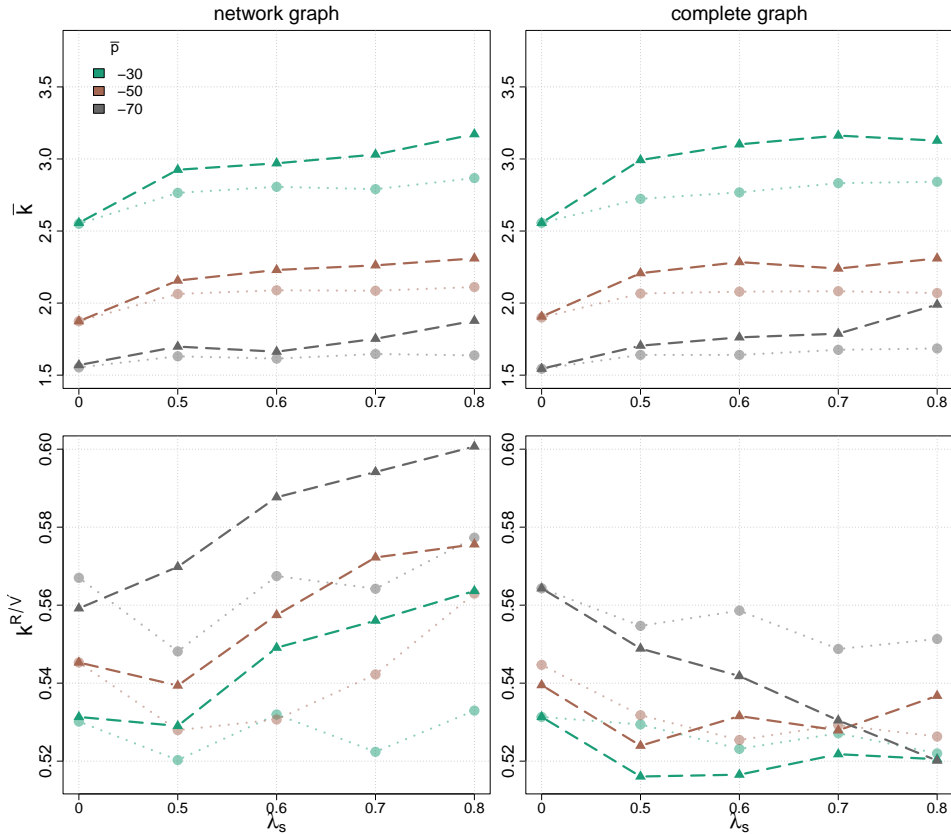


Figure 4: Average number of change points per time series  $\bar{k}$  (top row), and proportion of change points impacting redteam users  $k^{R/V'}$  (bottom row), assuming the network graph (left column) and the complete graph (right column), for different assumptions for the upper bounds for the lags - zero window (circles) and variable window (triangles), and for a collection of prior parameters  $\bar{p}$  (identified by distinct colours) and  $\lambda_s$ .

such that  $0 \leq m_i \leq k_i$ . Note that for each user  $i$ ,  $m_i$  increases with both the number of changepoints and their weights. Let

$$\bar{m} = \frac{1}{\text{card}(V')} \sum_{i \in V'} m_i, \quad m^{R/V'} = \frac{\sum_{i \in R} m_i}{\sum_{i \in V'} m_i} \quad (38)$$

be the average sum of changepoint weights per user and the proportion of changepoint weights associated to redteam users, respectively.

For each choice of graph and changepoint prior parameters, Figure 4 displays the estimated values of  $\bar{k}$  and  $k^{R/V'}$ , and Figure 5 displays the estimated values of  $\bar{m}$  and  $m^{R/V'}$  assuming  $\varpi = 48$ . As  $\bar{p}$  increases, weaker evidence is required to infer changepoints, and therefore, for each graph,  $\bar{k}$  and  $\bar{m}$  increase. As  $\lambda$  increases, the estimates for  $\bar{k}$  and  $\bar{m}$  tend to increase for each graph, but the estimates for  $k^{R/V'}$  and  $m^{R/V'}$  tend to increase only when assuming the network graph. This follows because the graphical changepoint model assuming the network graph successfully encodes prior knowledge that cyber attacks tend to correspond to coordinated activity across multiple users linked by network connectivity, and consequently, as  $\lambda$  increases, it detects weaker signals for behavioural changes that correspond to red team activity, whilst crucially limiting the number of false alerts. For the proposed model with the complete graph, all time series are connected, and therefore, as  $\lambda$  increases, weaker signals for changes are detected for red team activity but also for legitimate activity, which would impede fast identification of the attack.

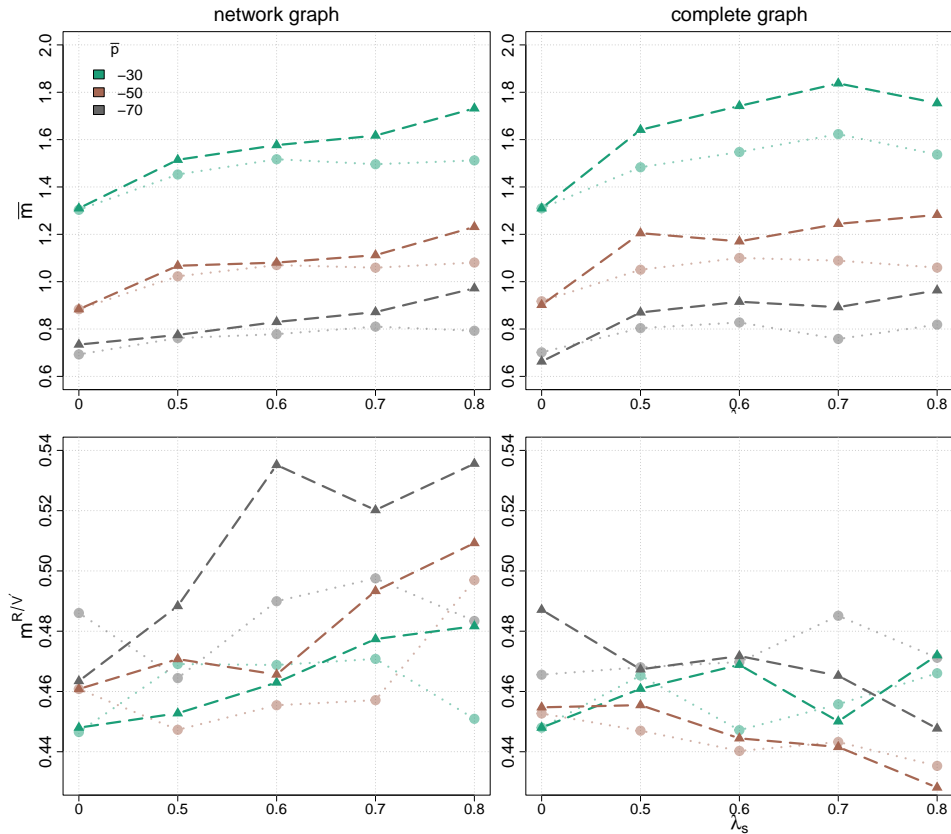


Figure 5: Estimated  $\bar{m}$  and  $m^{R/V'}$  (38), assuming the network graph (left column) and the complete graph (right column), for different assumptions for the upper bounds for the lags - zero window (circles) and variable window (triangles), and for a collection of prior parameters  $\bar{p}$  (identified by distinct colours) and  $\lambda_s$ .

Moreover, results show the benefits of the model extension which relaxes the assumption that signals for attacks are synchronous across users. As  $\lambda$  increases, when assuming the network graph, the increase of the estimates for  $k^{R/V'}$  and  $m^{R/V'}$  tend to be greater for the *variable window* scenario than for the *zero window* scenario. In contrast with the *zero window* scenario, the *variable window* scenario admits attacks may result in quasi-synchronous behavioural changes across the network, and consequently clusters of nearby but not necessarily synchronous weak signals for changepoints are detected across red team users.

The results show that, in comparison with the standard model for independent changepoints across time series, the proposed graphical changepoint model provides a flexible tool for cyber-analysts to incorporate expert knowledge in changepoint analysis for network monitoring, thereby facilitating network intrusion detection.

## 8. Discussion

This article considers a setting with  $N$  time series (1) subject to changepoints, where it is desirable to encode in the changepoint prior, by means of a graph  $G = (V, E)$  on  $N$  nodes corresponding to each of the time series, that pairs of time series  $(i, i') \in E$  are *a priori* more likely to be impacted by simultaneous changepoints. This setting is adapted to the application in cyber-security where each node in  $V$  corresponds to a time series representing the authentication activity of a network user, and an edge  $(i, i') \in E$  indicates that it is believed *a priori* that attackers may switch credentials between user  $i$  and user  $i'$  at any time of the data collection period, so that users  $i$  and  $i'$  are *a priori* more likely to be impacted by quasi-simultaneous behavioural changes.

However, for some applications, it might be restrictive to assume that prior beliefs on which time series are likely to be impacted by simultaneous changepoints do not vary over time. For example, consider the following application in cyber security. Using system log data, it can be of interest to monitor the process activity of computers, which may be subject to changes when attackers perform malicious activity such as the installation or the execution of malware. Moreover, attackers will typically need to communicate with compromised computers to simultaneously execute malicious commands on these computers. As a result, the process activity of computers  $i$  and  $i'$  are more likely to be subject to simultaneous changes when some source computer simultaneously communicates to both  $i$  and  $i'$ . For such a setting, it would be more suitable to specify a time series of graphs  $\{G_t = (V, E_t) \mid E_t \subseteq V \times V, t \geq 0\}$ , such that pairs of time series  $(i, i') \in E_t$  are *a priori* more likely to be impacted by simultaneous changepoints at time  $t$ . Each node in  $V$  would correspond to a time series representing the process activity of a computer in the network, and an edge  $(i, i') \in E_t$  would indicate that communication events occurred at time  $t$  from some source computer to both  $i$  and  $i'$ , so that computers  $i$  and  $i'$  are *a priori* more likely to be impacted by simultaneous behavioural changes at time  $t$ . For networks where many computers may leave or enter during the data collection period, a further model extension could consider relaxing the assumption that  $V$  is fixed, specifying a time series of graphs  $\{G_t = (V_t, E_t) \mid E_t \subseteq V_t \times V_t, V_t \subset \mathbb{N}, t \geq 0\}$  such that  $V_t$  is the node set of computers active in the network at time  $t$ . With the introduction of time-dependent edge weight parameters  $\lambda = (\lambda_{i,i',t})$  such that  $\lambda_{i,i',t} > 0$  if and only if  $(i, i') \in E_t$ , these model extensions would present no theoretical complication, with a straightforward adaption of the graphical changepoint prior and the proposed sampling strategy.

## Supplementary material

The *python* code and the data are available at [https://github.com/karl-hallgren/cp\\_on\\_graph\\_of\\_timeseries/](https://github.com/karl-hallgren/cp_on_graph_of_timeseries/)

## References

- Bardwell, L. and Fearnhead, P. (2017). Bayesian detection of abnormal segments in multiple time series. *Bayesian Analysis*, 12(1):193–218.
- Bardwell, L., Fearnhead, P., Eckley, I. A., Smith, S., and Spott, M. (2019). Most recent change-point detection in panel data. *Technometrics*, 61(1):88–98.
- Besag, J. and Green, P. J. (1993). Spatial statistics and Bayesian computation. *Journal of the Royal Statistical Society. Series B (Methodological)*, 55(1):25–37.
- Bolton, A. D. and Heard, N. A. (2018). Malware family discovery using reversible jump MCMC sampling of regimes. *Journal of the American Statistical Association*, 113(524):1490–1502.
- Bondy, J. A. and Murty, U. S. R. (1976). *Graph Theory with Applications*. Elsevier, New York.
- Carlin, B. P., Gelfand, A. E., and Smith, A. F. M. (1992). Hierarchical bayesian analysis of changepoint problems. *Journal of the Royal Statistical Society: Series C (Applied Statistics)*, 41(2):389–405.
- Chen, H. (2019a). Change-point detection for multivariate and non-euclidean data with local dependency. *arXiv:1903.01598*.
- Chen, H. (2019b). Sequential change-point detection based on nearest neighbors. *The Annals of Statistics*, 47(3):1381 – 1407.
- Chen, H. and Zhang, N. (2015). Graph-based change-point detection. *The Annals of Statistics*, 43(1):139 – 176.
- Chu, L. and Chen, H. (2019). Asymptotic distribution-free change-point detection for multivariate and non-Euclidean data. *The Annals of Statistics*, 47(1):382 – 414.
- Denison, D., Holmes, C., Bani, M., and Smith, A. (2002). *Bayesian Methods for Nonlinear Classification and Regression*. Wiley Series in Probability and Statistics, Chichester.
- Fearnhead, P. (2006). Exact and efficient bayesian inference for multiple changepoint. *Statistics and Computing*, 16(2):203–213.
- Fisch, A. T. M., Eckley, I. A., and Fearnhead, P. (2022). Subset multivariate collective and point anomaly detection. *Journal of Computational and Graphical Statistics*, 31(2):574–585.
- Gelman, A., Carlin, J. B., Stern, H. S., and Rubin, D. B. (2004). *Bayesian Data Analysis*. Chapman and Hall/CRC, 2nd ed. edition.
- Green, P. J. (1995). Reversible jump Markov chain Monte Carlo computation and Bayesian model determination. *Biometrika*, 82(4):711–732.
- Grundy, T. J., Killick, R., and Mihaylov, G. (2020). High-dimensional changepoint detection via a geometrically inspired mapping. *Statistics and Computing*, 30(99):1155–1166.
- Higdon, D. M. (1998). Auxiliary variable methods for Markov chain Monte Carlo with applications. *Journal of the American Statistical Association*, 93(442):585–595.
- Jeng, X. J., Cai, T. T., and Li, H. (2012). Simultaneous discovery of rare and common segment variants. *Biometrika*, 100(1):157–172.

- Johnson, T., Elashoff, R., and Harkema, S. (2003). A bayesian change-point analysis of electromyographic data: Detecting muscle activation patterns and associated applications. *Biostatistics*, 4(1):143–64.
- Kent, A. D. (2015). Cybersecurity data sources for dynamic network research. In *Dynamic Networks in Cybersecurity*. Imperial College Press, London.
- Lauritzen, S. L. (1996). *Graphical Models*. Oxford University Press, Oxford.
- Li, F. and Zhang, N. R. (2010). Bayesian variable selection in structured high-dimensional covariate spaces with applications in genomics. *Journal of the American Statistical Association*, 105(491):1202–1214.
- Metelli, S. and Heard, N. (2019). On Bayesian new edge prediction and anomaly detection in computer networks. *The Annals of Applied Statistics*, 13(4):2586 – 2610.
- Passino, F. S., Turcotte, M. J. M., and Heard, N. A. (2021). Graph link prediction in computer networks using poisson matrix factorisation. *The Annals of Applied Statistics*, page to appear.
- Punskaya, E., Andrieu, C., Doucet, A., and Fitzgerald, W. (2002). Bayesian curve fitting using mcmc with applications to signal segmentation. *IEEE Transactions on Signal Processing*, 50(3):747–758.
- Sexton, J. O., Storlie, C., and Neil, J. (2015). Attack chain detection. *Statistical Analysis and Data Mining*, 8(5):353–363.
- Swendsen, R. H. and Wang, J.-S. (1987). Nonuniversal critical dynamics in Monte Carlo simulations. *Phys. Rev. Lett.*, 58:86–88.
- Turcotte, M. (2014). Anomaly detection in dynamic networks. *PhD thesis, Imperial College London*.
- Wang, T. and Samworth, R. J. (2018). High dimensional change point estimation via sparse projection. *Journal of the Royal Statistical Society: Series B (Statistical Methodology)*, 80(1):57–83.

## Acknowledgements

The authors thank Niall Adams for stimulating discussions about this work. The authors acknowledge funding from EPSRC. Research presented in this article was supported by the Laboratory Directed Research and Development program of Los Alamos National Laboratory (New Mexico, USA) under project number 20180607ECR and Los Alamos National Laboratory.

## Appendices

### A. Motivational example: changepoint detection in cyber-security

This section gives further details on the motivational example discussed in Section 2.

#### A.1. Data processing

With the aim of modelling network activity that is human driven rather than high frequency and automated, the network authentication data, which are available online at <https://csr.lanl.gov/data/cyber1>, were filtered as follows: events involving the same pair of user and source computer more than 5 000 times were removed; computers that act as source computers for more than 300 distinct users were discarded. The resulting data involves 11 985 distinct users and 12 947 distinct source computers.

#### A.2. Limitations of changepoint independence across time series

To detect occurrences of malicious activity in the network, the authentication activity of each user is monitored via hourly counts of network logons per source computer. Figure 6 displays the first month of data for two distinct users that are linked on the network. The data are assumed to follow the changepoint model specified in Section 2. Assuming further that changepoints are independent with prior distribution given in (7), for a selection of Bernoulli parameters  $p$ , a sample from the posterior distribution of changepoints was obtained via the reversible jump MCMC algorithm proposed in Green (1995), adapted to discrete time changepoints. In Figure 7, for different Bernoulli parameters, the crosses and the red lines indicate the positions of Bayes changepoint estimates corresponding to the loss function  $L$  given in Definition 3 with  $\gamma = 40$ ; it is noticeable that  $p$  controls *a priori* the level of granularity of the segmentation of the data. The smaller  $p$ , the stronger the evidence required from the data to suggest a posteriori inferred changes. No choice of  $p$  seems satisfactory: choosing a small value for  $p$  will limit the number of false alerts due to noise and user specific legitimate activity; yet it will also prevent the detection of weak signals for changes shared by different users which are linked in the network, that may be of great interest.



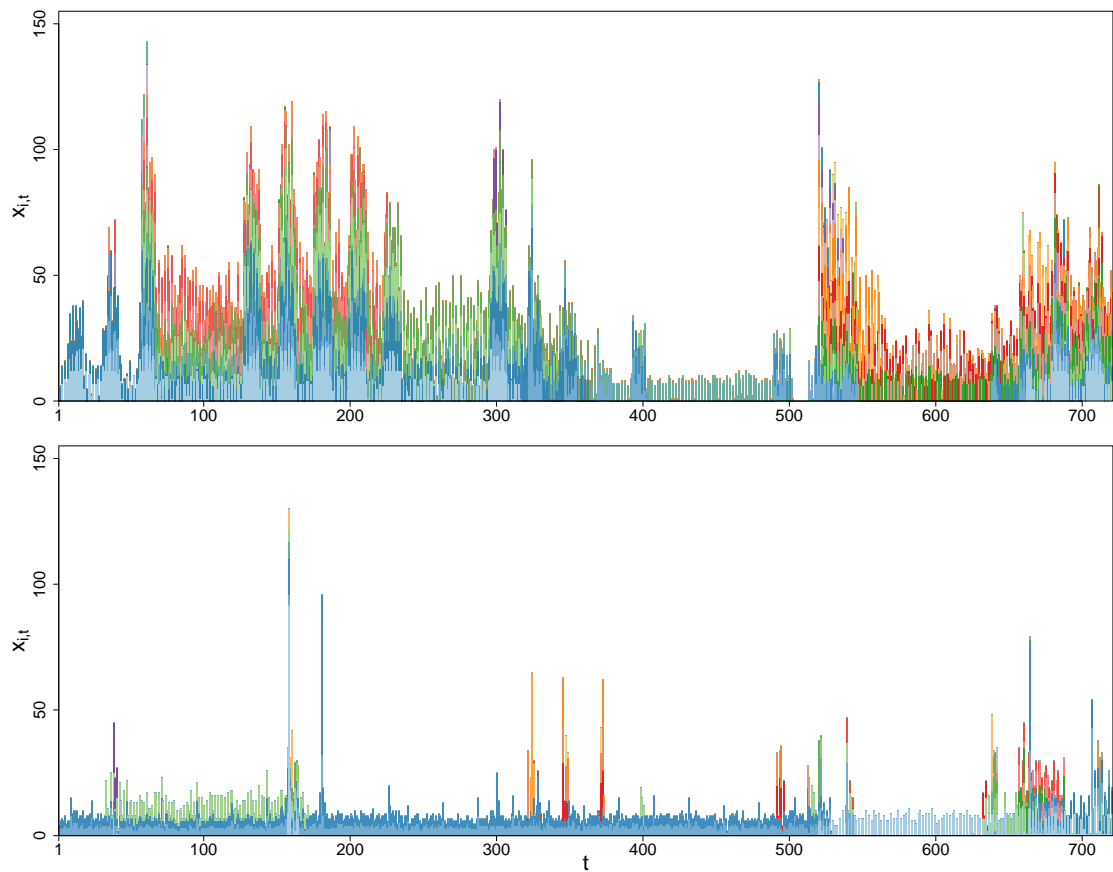


Figure 6: Hourly counts of network logons per source computer for two users over the first month of data collection. Source computers are identified by distinct colours. Top panel corresponds to user U342@DOM1, and bottom panel to user U86@DOM1.

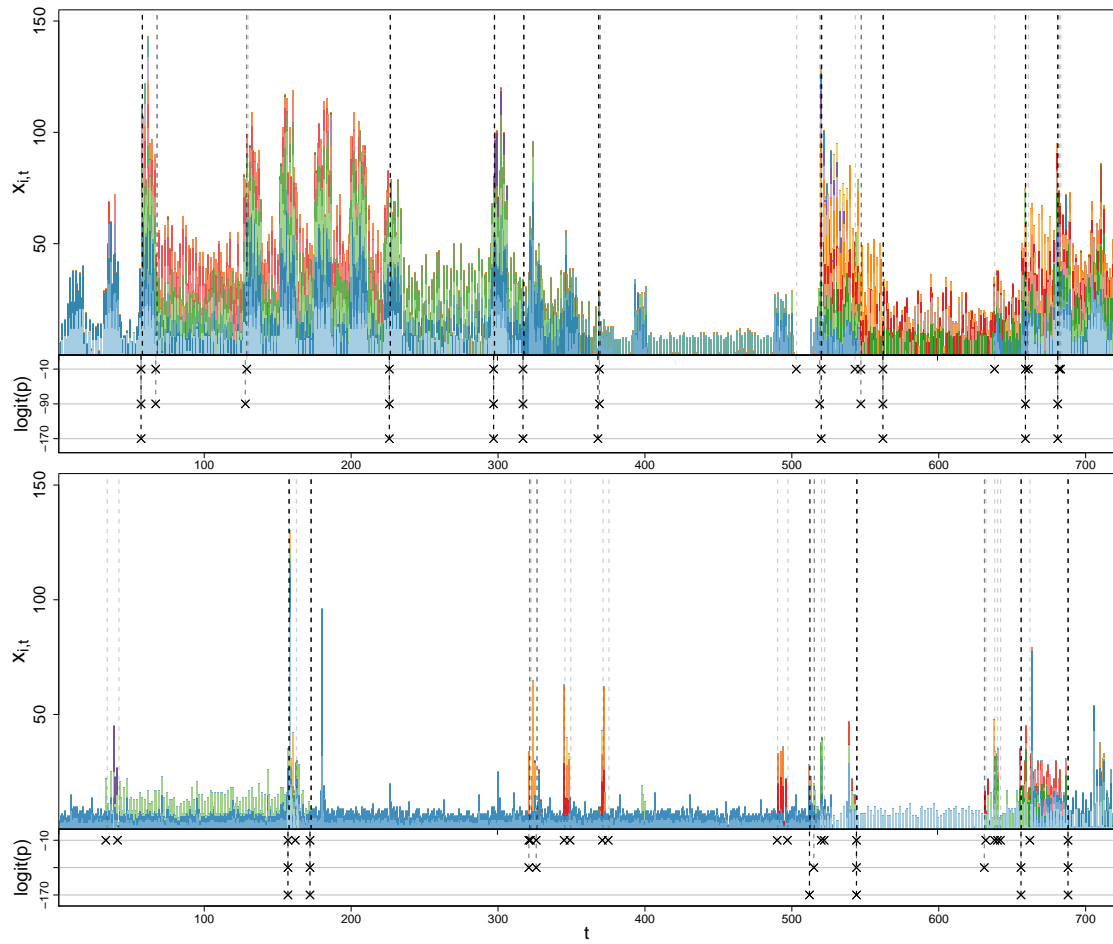


Figure 7: Hourly counts of network logons per source computer for two users over the first month of data collection; top panel corresponds to user U342@DOM1 and bottom panel to user U86@DOM1. Crosses indicate positions of Bayes changepoint estimates, according to the loss function  $L$  with  $\gamma = 40$ , corresponding to three different Bernoulli parameters  $p$ .

## B. Proof of Proposition 1

- (i) Let  $w \geq 0$ ,  $k \geq 0$  and  $\tau_{1:k} = (\tau_1, \dots, \tau_k) \in \mathcal{T}_k$ . We introduce some notations to facilitate the proof. For all  $0 \leq j \leq l \leq k$ , let

$$\Omega_{j:l} = \Omega_{j:l}(w, k, \tau_{1:k}) = \{d_{j:l} = (d_j, \dots, d_l) : \forall i, 0 \leq d_i < \rho(i, 0) = \min\{w + 1, T + 1 - \tau_i\}\}$$

and

$$\mathcal{Q}_{j:l} \equiv \mathcal{Q}_{j:l}(w, k, \tau_{1:k}) = \{d_{j:l} = (d_j, \dots, d_l) \in \Omega_{j:l} : \tau_j + d_j \geq \tau_{j+1} + d_{j+1} \geq \dots \geq \tau_l + d_l\}.$$

Note that  $\text{card}(\Omega_{j:l}) = \prod_{i=j}^l \rho(i, 0)$  and  $\text{card}(\mathcal{Q}_{j:l}) = Q(j, l - j)$  where  $Q$  is defined in (18).

It is immediate that if  $k = 0$  then (20) holds. If  $k = 1$  then  $\text{card}(\mathcal{D}(w, k, \tau_{1:k})) = \min\{w + 1, T + 1 - \tau_1\} = Z(1)$ . We show by induction that (20) holds for  $k > 1$ . If  $k = 2$  then

$$\begin{aligned} \text{card}(\mathcal{D}(w, k, \tau_{1:k})) &= \text{card}(\Omega_{1:2}) - \text{card}(\mathcal{Q}_{1:2}) \\ &= \rho(1, 0)\rho(2, 0) - Q(1, 1) \\ &= Z(1)Q(2, 0) - Z(0)Q(1, 1) \\ &= Z(2). \end{aligned}$$

Assume that (20) holds for  $k = 1, \dots, k' - 1$  for some  $k' > 2$ . We show that (20) holds for  $k = k'$ . We have

$$\begin{aligned} \text{card}(\mathcal{D}(w, k, \tau_{1:k})) &= \sum_{j=1}^k (-1)^{k-j} \text{card}(\{d_{1:k} \in \Omega_{1:k} : d_{1:(j-1)} \in \mathcal{D}(w, j-1, \tau_{1:(j-1)}), d_{j:k} \in \mathcal{Q}_{j:k}\}) \\ &= \sum_{j=1}^k (-1)^{k-j} \text{card}(\mathcal{D}(w, k-j, \tau_{1:(k-j)})) \text{card}(\mathcal{Q}_{j:k}) \\ &= \sum_{j=1}^k (-1)^{k-j} Z(j-1)Q(j, k-j) \\ &= Z(k). \end{aligned}$$

- (ii) Follows immediately from (16).

## C. Markov chain Monte Carlo inference

Section 5 proposed an auxiliary variable MCMC algorithm to sample from the graphical changepoint model. This section gives some indications on the time complexity of the algorithm and discusses possible extensions for settings where segment parameters cannot be marginalised.

### C.1. Time complexity and initialisation of the sampler

The move proposing to update auxiliary variables  $\mathbf{u} = (\mathbf{u}_t)$  from their full conditional distribution (23) is independent of preceding auxiliary variables in the sample chain and is accepted with probability 1. Moreover, the auxiliary variables  $\mathbf{u}$  provide a means to explore the changepoint parameter space but it is not of interest to store a sample from the posterior distribution of  $\mathbf{u}$ . Therefore, for all  $t$ , the sampling of the auxiliary parameters  $\mathbf{u}_t$  is performed only when a subsequent move depends upon  $\mathbf{u}_t$ , for example when a move proposes to update a cluster of changepoints at time  $t$ . As a result, the cost of updating auxiliary variables is at most  $\mathcal{O}(\text{card}(E))$  per iteration. Moreover, for the shift and the birth/death moves that propose to update changepoints for a cluster of time series  $C$ , an  $\mathcal{O}(T)$  Bayes factor calculation for the model in (6) is required for each time series in  $C$ . If  $\delta = 0$  then  $\text{card}(C) = 1$ ; otherwise, the expected size of the cluster  $1 \leq \text{card}(C) \leq N$  will tend to increase with  $N$ . Hence, the computational cost of moves proposing to update changepoints is at most  $\mathcal{O}(TN)$ .

To speed-up the convergence of the sampler, we may consider the following initialisation of the sample chain: latent changepoints are set to be the optimal Bayesian estimates, according to the loss function later specified in Definition 3, corresponding to the standard model with independent changepoints across time series with prior  $\pi(\mathbf{k}, \boldsymbol{\tau}|p)$ , obtained in parallel for each time series; initial lags, upper bounds for lags and auxiliary variables are set to 0. As a result, the burn-in for the sampler begins with a sensible positioning of changepoints at a limited cost: no iterations for the burn-in of the joint sampling of changepoints across time series are wasted identifying strong signals for changepoints, relative to  $\bar{p}$ .

Section D.3 presents results of a simulation study demonstrating the feasibility of the proposed inference via MCMC for a range of  $N$  and  $T$  that can correspond to realistic scenarios. For high-dimensional applications where the time until reaching suitable convergence can be prohibitively long, future work could examine analytical approximations to the posterior distribution of changepoints, for example via variational methods (Blei et al., 2017).

### C.2. Possible sampling algorithm extensions for segment parameters

The proposed sampling strategy assumes that segment parameters can be marginalised to compute the conditional likelihood of the data given changepoints,  $\mathcal{L}(\mathbf{x}|\mathbf{k}, \boldsymbol{\tau})$ . Although this assumption is appropriate in many applications, as discussed in Section 3.1, it will not always be the case; for example when segment parameters are dependent across segments (Chib, 1998; Peluso et al., 2019; Fearnhead and Liu, 2011). If segment parameters cannot be marginalised, the proposed reversible jump MCMC algorithm can be adapted to sample segment parameters alongside changepoint parameters as in Green (1995): a move is introduced to sample segment parameters conditional on changepoints; the moves proposing updated changepoint parameters are extended to propose suitable parameters for the segments that are affected by the proposed change of changepoint parameters; note that the proposal distributions for segment parameters depend on the segment model of interest.

Moreover, an interesting model extension of the changepoint model in (6) consists in specifying that segment parameters may be shared across segments: each segment parameter  $\theta_{i,j}$  can take one of a finite, but unknown, number of states. Segments that share the same parameter, possibly across time series, are said to be under the same regime, and regime parameters can still

be marginalised for conjugate probability models (Bolton and Heard, 2018). In this setting, the proposed MCMC algorithm would need to be adapted to sample the changepoint parameters, the number of regime and a regime for each segment following Bolton and Heard (2018).

## D. Simulation study

This section presents a simulation study to demonstrate the model for dependent changepoints proposed in Section 4 and the sampling strategy discussed in Section 5. In particular, various graphs and changepoint parameters are considered to illustrate the flexibility of the proposed model. Moreover, the proposed model is compared with the standard model for independent changepoints, which assumes all edge weight parameters are null (10), and with MVCAPA (Fisch et al., 2022), which can borrow strength across multiple time series to detect synchronous changepoints across a subset of the time series but assumes *a priori* changepoint locations are exchangeable across time series.

### D.1. Synthetic data

Synthetic data for the simulation study were sampled according to the changepoint model for  $N$  time series each of length  $T$  defined in (6) with, for all  $i$ ,  $f_i(\cdot | \theta_{i,j})$  corresponding to  $\text{Poisson}(\theta_{i,j})$ , for a range of values of  $N \in \{30, 130, 230, 330\}$  and  $T \in \{300, 3\,300, 6\,300, 9\,300\}$ .

For simulating data, let  $C \subset \{1, \dots, N\}$  be a non-empty subset of the time series indices, and let  $\bar{C}$  be the set complement such that  $C \cup \bar{C} = \{1, \dots, N\}$ . Then let  $k_i = k$  if  $i \in C$ , where  $k$  is uniformly sampled from  $\{1, \dots, 7\}$ , and  $k_i = 0$  otherwise, such that  $C$  denotes those series which experience changepoints while those in  $\bar{C}$  are not impacted by changepoints. The impact of encoding prior information on the dependence structure of changepoints across time series on a graph will be investigated by means of further divisions of the set  $C$  into subsets. We fixed  $C = C_1 \cup C_2 \cup C_3$  for some disjoint sets  $C_1 = \{1, 2, \dots, \lfloor N/5 \rfloor\}$ ,  $C_2 = \{N, N-1\} \cup \{N - \lfloor N/5 \rfloor, N - \lfloor N/5 \rfloor - 1\} \cup \{N - 2\lfloor N/5 \rfloor, N - 2\lfloor N/5 \rfloor - 1\}$  and  $C_3 = \{\lfloor N/2 \rfloor - 1\}$ . As illustrated in Figure 8 for  $N = 30$  time series, according to both the  $6 \times 5$  lattice graph or the 2-chain graph, the elements of  $C_1$  and  $C_2$  cluster according to the graph, whereas the single element of  $C_3$  has no neighbours in  $C$  so that it is isolated in the graph. Moreover, different scenarios for changepoint positions were considered: for all  $i \in C$ , we set  $\tau_{i,j} = \lfloor jT/(k_i + 1) \rfloor + v_{i,j}$ , where  $v_{i,j}$  is sampled from  $\{-v, 0, v\}$ , for increasing levels of asynchrony for the changepoints  $v \in \{0, 5, 10, 15\}$ . For the scenario with  $v = 0$ , changepoints are synchronous. Finally, for all  $i \in C$ , the signal strength for changepoints may be quantified by

$$\mu_i = \frac{1}{k_i} \sum_{j=1}^{k_i} \log \left\{ E \left( \frac{\mathcal{L}_i(\tau_{j-1}, \tau_j) \mathcal{L}_i(\tau_j, \tau_{j+1})}{\mathcal{L}_i(\tau_{j-1}, \tau_{j+1})} \right) \right\}, \quad (39)$$

where  $\mathcal{L}_i$  is defined in (5). For all  $i \in V$  and  $j = 1, \dots, k_i + 1$ , let  $\theta_{i,j} = 1000$  if  $j$  is odd and  $\theta_{i,j} = \theta(\mu, k_i)$  if  $j$  is even, where  $\theta(\mu, k_i)$  is such that  $\mu_i = \mu$  for some  $\mu > 0$  if  $i \in C$ . The greater  $\mu$ , the greater  $\theta(\mu, k_i)$ . A range of values for  $\mu$  was considered and Monte Carlo estimations were computed for the corresponding parameters  $\theta(\mu, k_i)$ . Ten simulations were performed for each combination of the parameters  $N, T, v$  and  $\mu$ .

### D.2. Changepoint inference

For each simulation, different models were used to infer changepoint estimates from the data: the proposed changepoint model assuming different prior beliefs on the dependence structure of changepoints, and MVCAPA (Fisch et al., 2022). MVCAPA detects collective anomalies in multiple time series such that, by means of lags, anomalies are not necessarily aligned, and it

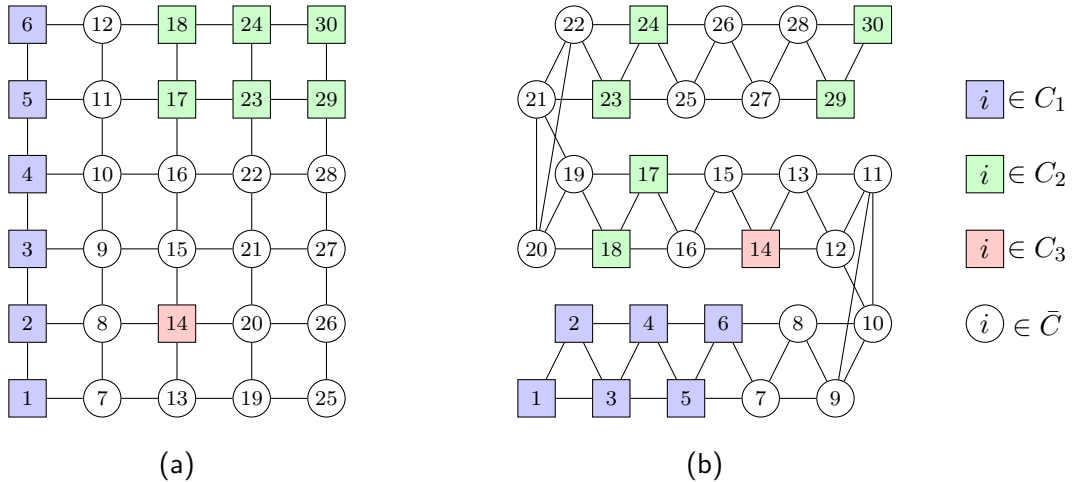


Figure 8: Graphs of time series indices  $i \in \{1, \dots, 30\}$  representing different dependence structures of changepoints discussed in Section 4.2; panels (a) and (b) correspond to a  $6 \times 5$  lattice and a 2-chain, respectively. For all  $i$ , circles indicate  $i \in \bar{C}$  and squares indicate  $i \in C$ ; colours blue, green and red indicate that  $i \in C_1$ ,  $C_2$  and  $C_3$ , respectively.

relies on the choice of a penalty parameter that controls the level of evidence required to flag a changepoint. We used the implementation from the *R* package *anomaly* to fit MVCAPA, without lags and with lags (fixing the maximal lag to 30), with the default penalty rescaled by a constant  $\phi$  for various  $\phi > 0$ .

For the proposed changepoint model (6), it is assumed that, for all  $i$ ,  $f_i(\cdot | \theta_{i,j})$  corresponds to  $\text{Poisson}(\theta_{i,j})$  and  $\theta_{i,j} \sim \Gamma(100, 0.1)$ , given the proposed changepoint prior for a collection of changepoint prior parameters. Different dependent structures for changepoints across time series were used, as illustrated in Figure 8: the dependence structure corresponding to the  $r$ -chain graph for time series indices, for  $r \in \{2, 4, 6, \dots, N/2\}$ , given in Section 4.2.2; the dependence structure corresponding to a  $6 \times 5$  lattice graph, given in Section 4.2.1, for scenarios with  $N = 30$  time series; and the dependence structure corresponding to a complete graph given in Section 4.2.3. Moreover, different changepoint prior parameters  $\bar{p} \in \{-60, -70, \dots, -130\}$  and  $\lambda = \lambda_s |\bar{p}|/n$  with  $\lambda_s \in \{0, 0.2, \dots, 0.8\}$ , where  $n$  denotes the maximum degree of  $G$ . Note that models with  $\lambda = 0$  correspond to the standard model for independent changepoints (10). Furthermore, three different scenarios are considered for the upper bounds  $w$  for the lags: for the *fixed window* scenario, we fix  $w_i = 30$  for all  $i$ ; for the *variable window* scenario, it is assumed *a priori* that  $w_i \sim \text{Geometric}(0.9)$  for all  $i$ ; for the *zero window* scenario, we fix  $w_i = 0$  for all  $i$ , which is equivalent to assuming the prior for synchronous dependent changepoints defined in (9).

For each combination of changepoint prior parameters, five independent samples of size  $2000N$  were obtained from the posterior distribution of changepoints, via the MCMC algorithm proposed in Section 5.1, with a burn-in of  $300N$  iterations. Samples were thinned at a rate of one per  $N$ . Note that, when  $\lambda > 0$ , we set  $\delta_0 = 0.5$ ,  $\delta_1 = 1$ ,  $\delta_2 = 30$  for the prior of the parameter  $\delta$ , so that linked time series indices are expected to bond with probability 0.5 when  $\delta > 0$ , according to (23).

It is of interest to compare the role of graph-based hyperparameters for the proposed model with the role of  $\phi$  for MVCAPA when estimating changepoints. MVCAPA and the proposed model provide changepoint estimates for each time series. To compare inferred changepoints with respect to the changepoints used to simulate data for each time series, both the mean squared error (MSE) for the number of changepoints and the loss  $L$  defined in Definition 3, fixing  $\gamma = 40$ , which takes into account both the number and the positions of changepoints, are considered.

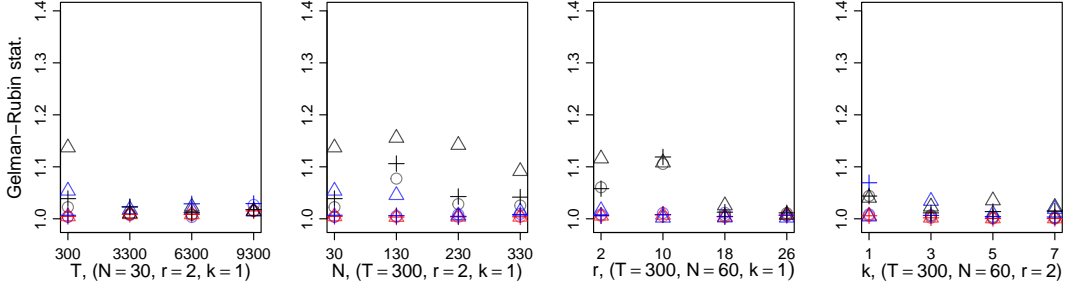


Figure 9: Average Gelman-Rubin statistics for independent samples obtained via the proposed MCMC algorithm for a collection of scenarios:  $\lambda_s = 0$  (Red);  $\lambda_s = 0.2$  (Blue);  $\lambda_s = 0.6$  (Black); zero window (Cross); fixed window (Circle); variable window (Triangle).

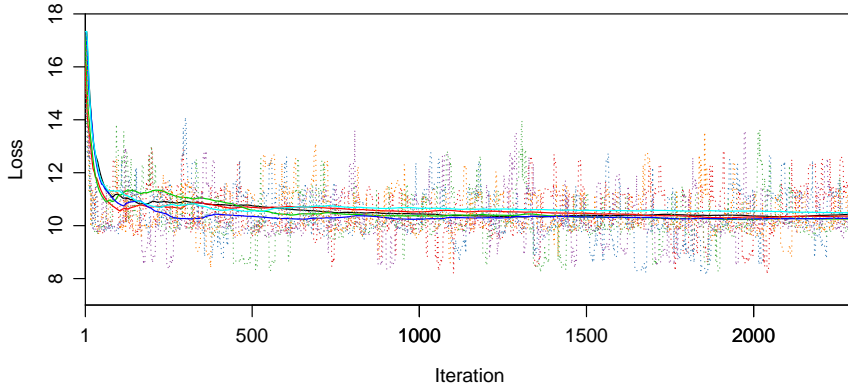


Figure 10: Five independent chains of the value of the loss function obtained via MCMC (dotted lines), with corresponding average loss function value (solid lines).

### D.3. MCMC diagnostics and runtime

The Gelman-Rubin test (Gelman and Rubin, 1992) is used to assess the convergence of the sampler by comparing between-chain and within-chain variances of multiple chains. For each simulation and choice of changepoint prior parameters, the Gelman and Rubin test statistic, which was computed for the five independent chains of the value of the loss function (32) obtained via MCMC, was less than 1.2, suggesting that the sampler has converged; see Figure 9 for a breakdown of results. Moreover, to illustrate the good mixing properties of the sampler, one simulation for the scenario with  $N = 30$ ,  $T = 300$ ,  $k = 1$ ,  $v = 10$  and  $\mu = 90$  is considered. Figure 10 displays five independent chains of changepoint loss obtained via the proposed MCMC algorithm assuming the 2-chain graph for time series with  $\bar{p} = -80$ ,  $\lambda_s = 0.6$ ; it is apparent that the chains converge to the same changepoints with good mixing properties.

Figure 11 displays the average runtime of an iteration of the MCMC algorithm, implemented in *Python* and run on a 2.6GHz Intel Core i7 processor, for a collection of scenarios assuming an  $r$ -graph for the dependence structure of the changepoints. Results support the discussion in Section C.1. The runtime is linear in the number of observations  $T$ . When changepoints are dependent with  $\lambda > 0$  and  $\delta > 0$ , the runtime is linear in the number of time series  $N$  and in the number of edges in  $G$ , which is  $2r$  for the  $r$ -chain graph. However, when  $\lambda = 0$ , we update a single time series at each iteration of the algorithm, so that the runtime is independent of  $N$  and  $r$ . The runtime does not increase with the number of changepoints  $k$ . Moreover, the runtime per iteration increases for the extended model with lags, for fixed and unknown windows, since lags must be proposed alongside latent changepoints.

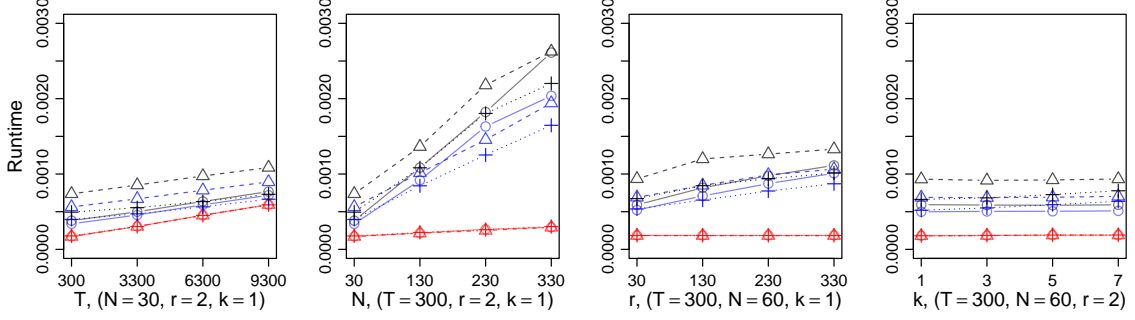


Figure 11: Average runtime in seconds per iteration for the MCMC algorithm for a collection of scenarios:  $\lambda_s = 0$  (Red);  $\lambda_s = 0.2$  (Blue);  $\lambda_s = 0.6$  (Black); *zero window* (Cross); *fixed window* (Circle); *variable window* (Triangle).

#### D.4. Changepoint estimation results

This section discusses results of the simulation study for scenarios with  $N = 30$  and  $T = 300$  to demonstrate the merit of the graphical changepoint prior that induces a changepoint model combining weak signals for changepoints across clusters of time series in  $G$ , in comparison with the standard model for independent changepoints and MVCAPA.

##### D.4.1. Detection of clusters of changepoints on a graph of time series

First, we focus on demonstrating the role of the graph  $G$  and the changepoint parameters  $p$  and  $\lambda$  using simulations corresponding to scenarios with  $v = 0$  for synchronous changepoints and with  $\mu = 90$ . Figure 12 displays the MSE for  $k_i$  for time series  $i$  in clusters  $C_1, C_2, C_3$ , for the graphical changepoint models and for MVCAPA as a function of changepoint prior parameters.

For each graphical changepoint model, as  $\bar{p}$  decreases, stronger evidence is required to infer changepoints and therefore the MSE for  $k_i$  increases for  $i \in C_1, C_2, C_3$ . The impact of  $\lambda$  depends on the graph-based dependence structure. Consider the 2-chain and the  $6 \times 5$  lattice graphs for  $N = 30$  time series as illustrated in Figure 8: for  $i \in C_3$ , the simulated changepoint is isolated on the graphs, whereas for  $i \in C_1, C_2$  the simulated changepoints cluster on the graphs. As a result, as  $\lambda$  increases, the interaction parameter  $\lambda$  has no impact on the MSE for  $k_i$  for  $i \in C_3$ , and the MSE for  $k_i$  decreases for  $i \in C_1, C_2$  because weaker signals for changepoints, relative to  $\bar{p}$ , are combined across time series which cluster according to the graphs. The MSE for  $k_i$  for  $i \in \bar{C}$  is close to 0 for all scenarios, showing that an increase in  $\lambda$  does not lead to changepoint overfitting.

However, both for the graphical changepoint model with the complete graph and for MVCAPA, changepoint locations are assumed to be exchangeable across time series, and therefore the impact of changepoint prior parameters are identical for all time series  $i \in C_1, C_2$  and  $C_3$ . The simulated changepoints are all connected on the complete graph, and consequently, as  $\lambda$  increases, the MSE for  $k_i$  decreases for  $i \in C_1, C_2, C_3$  for the graphical changepoint model with a complete graph. For MVCAPA, as the penalty term  $\phi$  increases, the MSE for  $k_i$  decreases for time series  $i \in C_1, C_2, C_3$ .

For further evidence that the posterior distribution adapts to the dependence structure for changepoints specified *a priori* via the graph  $G$ , observe that, as  $\lambda$  increases, for the dependence structure induced by the 2-chain, the MSE for  $k_i$  is lower for  $i \in C_1$  than for  $i \in C_2$ , since time series  $i \in C_1$  have a greater proportion of neighbour time series impacted by changepoints than time series  $i \in C_2$ , as illustrated in Figure 8. For the dependence structure induced by the lattice, however, time series  $i \in C_1$  have a lower proportion of neighbour time series impacted by changepoints than time series  $i \in C_2$ , so that the MSE for  $k_i$  is greater for  $i \in C_1$  than for



$i \in C_2$ . Moreover, as  $\lambda$  increases, the MSE for  $k_i$  for  $i \in C_1$  is lower for the 2-chain graph than for the complete graph, whereas the MSE for  $k_i$  for  $i \in C_2$  is greater for the 2-chain graph than for the complete graph. This follows because the proportion of neighbour time series impacted by changepoints is lower for the complete graph than the 2-chain graph for time series  $i \in C_1$ , but larger for time series  $i \in C_2$ .

The roles of  $G$ ,  $p$  and  $\lambda$  are the same when detecting asynchronous changepoints. It is apparent in Figure 13, that displays the MSE for the number of changepoints for the scenarios with  $v = 10$  for asynchronous changepoints and assuming the *fixed window* scenario for the graphical changepoint models. Results are similar for other levels of asynchrony  $v$ .

For other signal strengths considered in the experiment  $\mu \in \{55, 120\}$ , results are similar to results for the scenario where  $\mu = 90$  when it comes to the role of changepoint prior parameters. Yet, by considering results for the dependence structure corresponding to the 2-chain displayed in Figure 14, we note that, as the signal strength increases, the region of low MSE for  $k_i$  for time series  $i \in C_1, C_2$  translates along the  $\bar{p}$  axis on the  $\bar{p}, \lambda$ -plane.

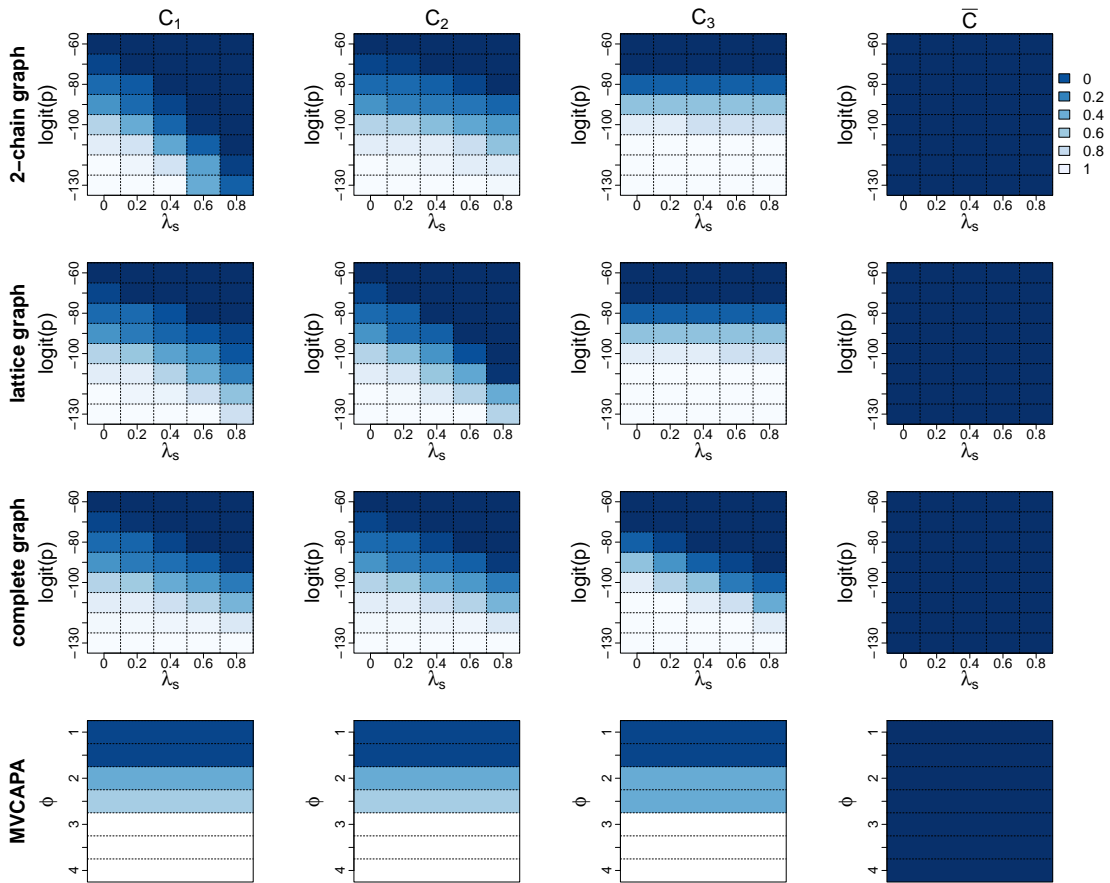


Figure 12: Mean squared error for the number of changepoints  $k_i$  for time series  $i$  in clusters  $C_1, C_2, C_3, \bar{C}$ . Top rows: estimates for the graphical changepoint model assuming the 2-chain graph, the lattice graph and the complete graph, as a function of  $\bar{p} = \text{logit}(p)$  and  $\lambda_s$ . Bottom row: estimates for MVCAPA as function of  $\phi$ . Results correspond to scenarios with  $v = 0$  and  $\mu = 90$ .

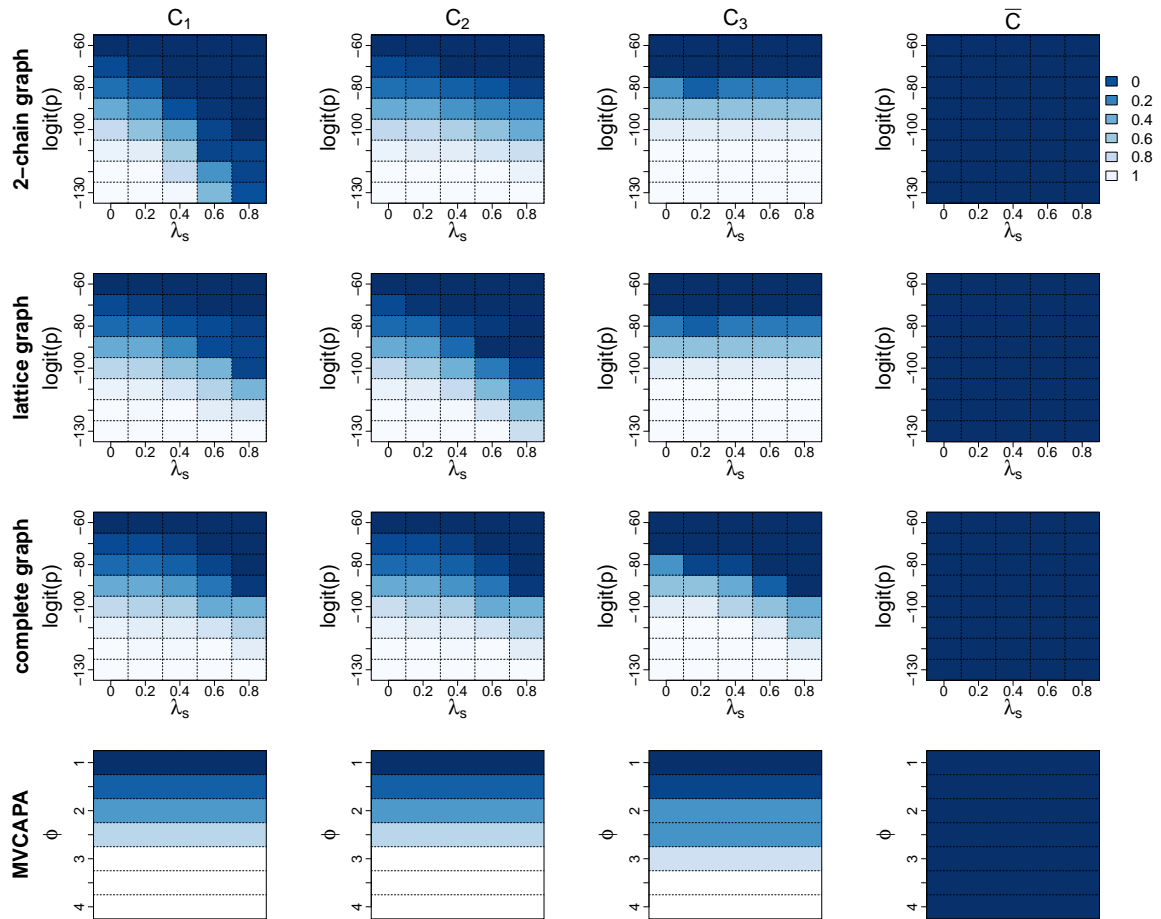


Figure 13: Mean squared error for  $k_i$  for time series  $i$  in clusters  $C_1, C_2, C_3, \bar{C}$ . Top rows: estimates for the graphical changepoint model assuming the 2-chain graph, the lattice graph and the complete graph, as a function of  $\bar{p} = \text{logit}(p)$  and  $\lambda_s$ . Bottom row: estimates for MVCAPA as function of  $\phi$ . Results correspond to scenarios with  $v = 10$  and  $\mu = 90$ .

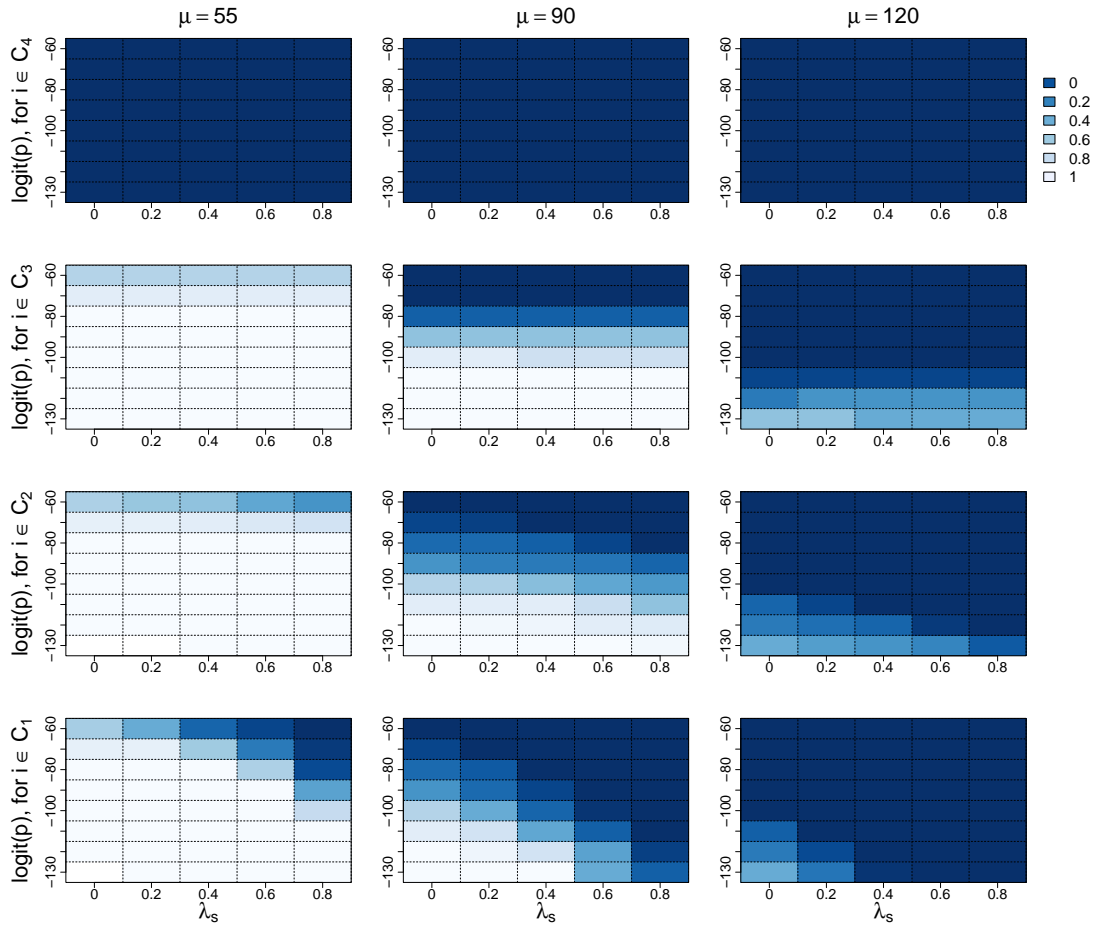


Figure 14: Mean squared error for  $k_i$  for times series  $i \in C_1, C_3$ , given the 2-chain graph based dependence structure for changepoints, as a function of  $\bar{p} = \logit(p)$  and  $\lambda_s$ , and for different strength signals for changepoints  $\mu \in \{55, 90, 120\}$ .

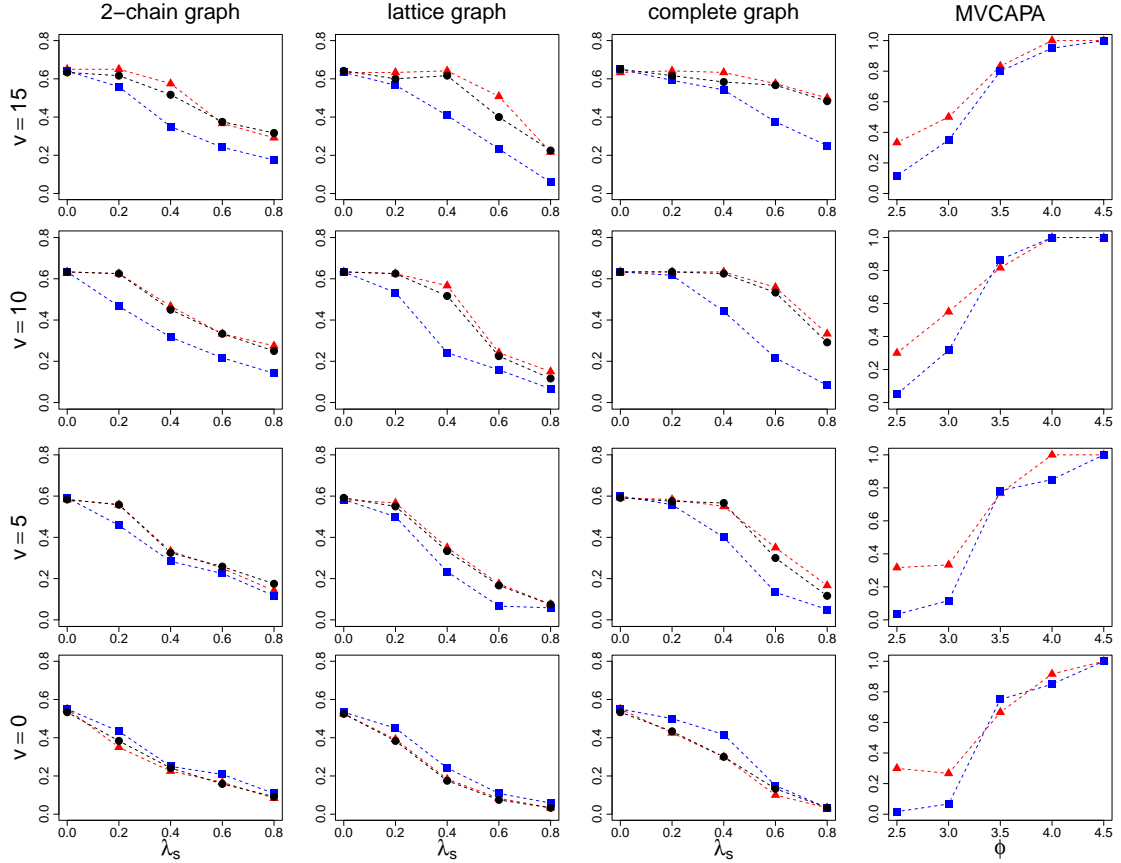


Figure 15: Mean squared error for  $k_i$  for time series  $i \in V$  for increasing levels of changepoint asynchrony  $v$ . Left columns: graphical changepoint models for different assumptions for the upper bounds for the lags - *fixed window* (blue squares), *variable window* (black circles), and *zero window* (red triangles). Right column: MVCAPA with lags (blue squares) and without lags (red triangles).

#### D.4.2. Detection of quasi-synchronous changepoints

This section discusses results for scenarios with increasing levels of asynchrony for changepoints  $v \in \{0, 5, 10, 15\}$  and with  $\mu = 90$ . Recall changepoints are synchronous for scenarios with  $v = 0$ .

Figure 15 displays the MSE for  $k_i$  for  $i \in V$  for the graphical changepoint model assuming different assumptions for the upper bounds for the lags, different graphs  $G$  and edge weight parameters  $\lambda$ , and  $\bar{p} = -90$ . As the level of asynchrony of the changepoints  $v$  increases, the MSE for  $k_i$  tends to be greater for the *zero window* scenario than for the *fixed window* or the *variable window* scenarios. Hence, there is merit in relaxing the assumption that signals for changepoints must be synchronous. In particular, the MSE for  $k_i$  tends to be greater for the *variable window* than for the *fixed window* scenarios, therefore encouraging practitioners to specify fixed time windows when possible. Moreover, as the interaction parameter  $\lambda$  increases, the decrease in MSE tends to be greater for the 2-chain graph and the lattice graph than for the complete graph. This follows because for time series  $i \in C$  the proportion of neighbour time series impacted by changepoints is greater for the lattice graph and the 2-chain graph than for the complete graph. Figure 15 also displays results for MVCAPA with and without lags. As the level of asynchrony for changepoints  $v$  increases, the MSE tends to increase for MVCAPA without lags. Results also show that, in contrast with the graphical changepoint models, specifying fixed lags when simulated changepoints are synchronous may adversely affect the performance of MVCAPA.

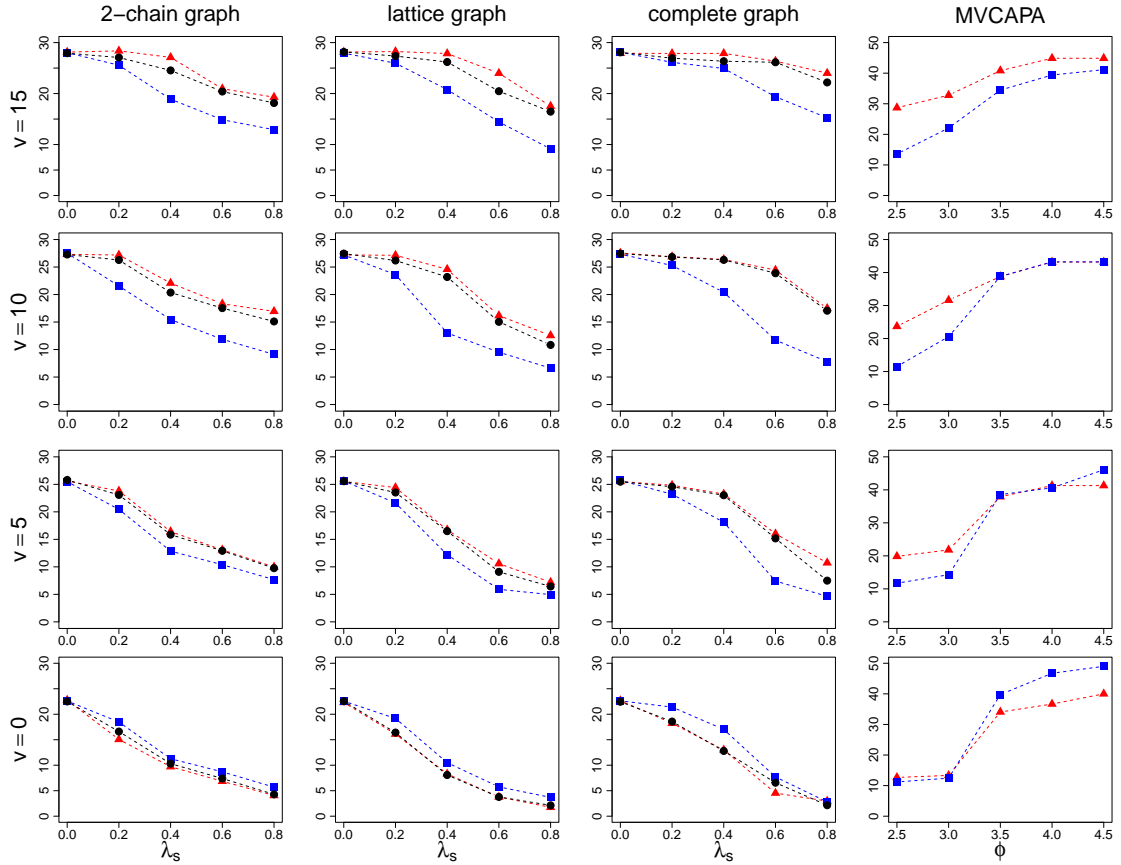


Figure 16: Monte Carlo estimates of the expected loss  $L$  for time series  $i \in V$  for increasing levels of changepoint asynchrony  $v$ . Left columns: graphical changepoint models for different assumptions for the upper bounds for the lags - *fixed window* (blue squares), *variable window* (black circles), and *zero window* (red triangles). Right column: MVCAPA with lags (blue squares) and without lags (red triangles).

Figure 16 displays the results discussed in Section D.4.2 in terms of the expected loss  $L$ , showing the model extensions have merit both in terms of detecting asynchronous signals for changepoints and correctly estimating the positions of these signals.

As shown in Figure 17, the role of changepoint lags is the same when assuming different  $\bar{p}$ .

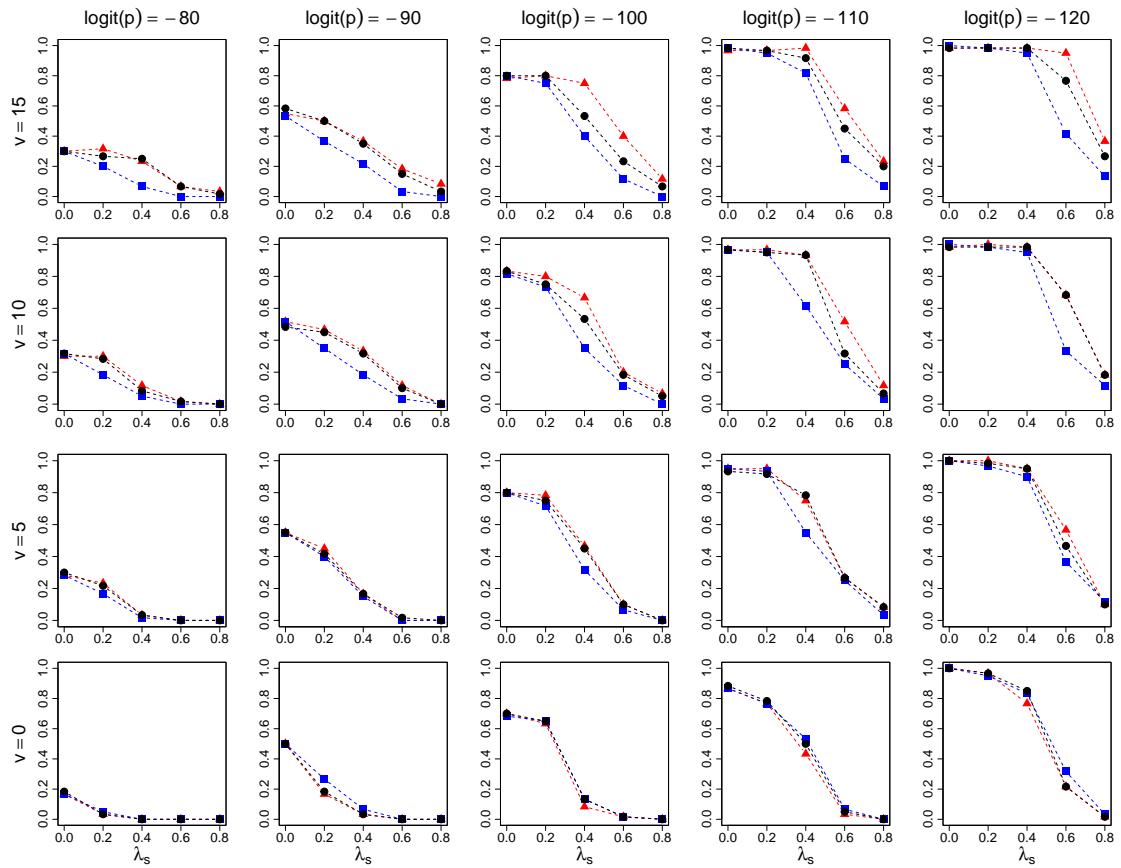


Figure 17: Mean square error for  $k_i$  for time series  $i \in C_1$ , given the 2-chain dependence structure for changepoints, corresponding to different assumptions for the upper bounds for the lags - *fixed window* (blue squares), *variable window* (black circles), and *zero window* (red triangles) - for increasing levels of asynchrony of the changepoints  $v$ , and for a collection of changepoint prior parameters  $p, \lambda_s$ .

### D.4.3. Importance of auxiliary variables

We demonstrate that it is pertinent to use auxiliary variables to sample from the posterior distribution of dependent changepoints, as discussed in Section 5. For the simulated data discussed in Section D.4.1, which correspond to scenarios with  $v = 0$  and  $\mu = 90$ , changepoints were sampled via MCMC as described in Section D.2, but now with  $\delta = 0$ , meaning the parameter space was not augmented with auxiliary variables (24). Figure 18 compares the MSE for  $k_i$  from samples obtained with and without auxiliary variables, for  $i \in C_1, C_2$ , and for the 2-chain and the lattice graph based dependence structures for changepoints. Without auxiliary variables, the MCMC algorithm fails to explore the state space of changepoints so that the number of changepoints tend to be underestimated; in other words, clusters of weak signals for changepoints across time series tend to be overlooked. The difference in performance, in favour of the MCMC algorithm making use of auxiliary variables, is particularly important when interaction parameters are large and weak signals for changepoints correspond to time series whose indices induce subgraphs with a large number of edges, as for  $i \in C_1$  given the 2-chain dependence structure in Figure 18.

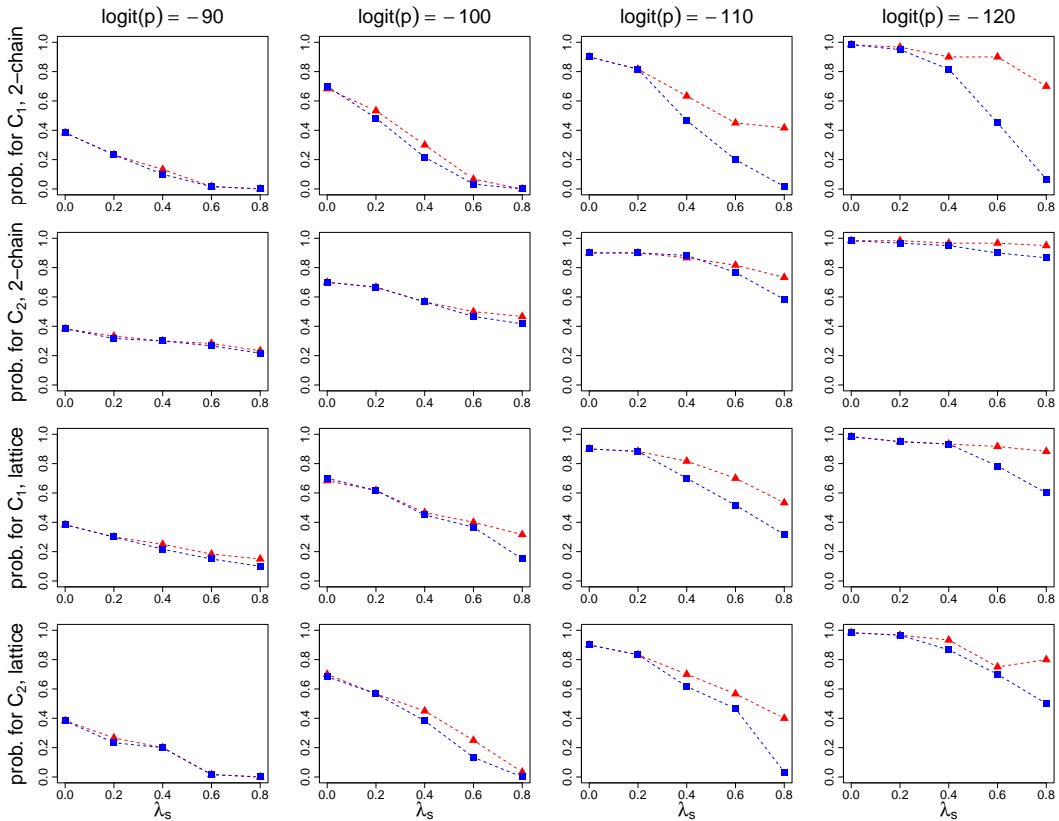


Figure 18: Mean squared error for  $k_i$  for time series  $i \in C_1, C_2$ , obtained via simulations with auxiliary variables (blue squares) and without auxiliary variables (red triangles), for the 2-chain and the lattice graph based dependence structures, and for a collection of changepoint prior parameters  $p$  and  $\lambda_s$ .

## References

- Blei, D. M., Kucukelbir, A., and McAuliffe, J. D. (2017). "Variational inference: A review for statisticians." *Journal of the American Statistical Association*, 112(518): 859–877.
- Bolton, A. D. and Heard, N. A. (2018). "Malware family discovery using reversible jump MCMC sampling of regimes." *Journal of the American Statistical Association*, 113(524): 1490–1502.
- Chib, S. (1998). "Estimation and comparison of multiple change-point models." *Journal of Econometrics*, 86(2): 221–241.
- Fearnhead, P. and Liu, Z. (2011). "Efficient Bayesian analysis of multiple changepoint models with dependence across segments." *Statistics and Computing*, 21(2): 217–229.
- Fisch, A. T. M., Eckley, I. A., and Fearnhead, P. (2022). "Subset Multivariate Collective and Point Anomaly Detection." *Journal of Computational and Graphical Statistics*, 31(2): 574–585.
- Gelman, A. and Rubin, D. B. (1992). "Inference from iterative simulation using multiple sequences." *Statistical Science*, 7(4): 457 – 472.
- Green, P. J. (1995). "Reversible jump Markov Chain Monte Carlo computation and Bayesian model determination." *Biometrika*, 82(4): 711–732.
- Peluso, S., Chib, S., and Mira, A. (2019). "Semiparametric multivariate and multiple change-point modeling." *Bayesian Analysis*, 14(3): 727 – 751.